

$\delta^{18}\text{O}$. Seasonal patterns were also evident, with lower isotopic values during winter due to cold-temperature isotopic fractionation and remote moisture sources and more positive values in summer as a result of convective storms and evaporation. During the drier year (2024) with a reduced moisture surplus, river systems relied more on stored winter precipitation, emphasizing the buffering role of groundwater. Deuterium excess (d-excess) values further showed regional differences in moisture sources. Higher d-excess in western Maryland pointed to potential lake-effect precipitation derived from the Laurentian Great Lakes and long-distance transport, whereas lower values in the east reflected enhanced local evaporation. These findings establish a regional baseline that enhances our understanding of hydrological and climatic controls of river-water isotope values across Maryland. They also imply that a reduction in winter precipitation could diminish groundwater recharge and baseflow, affecting dry-season water availability. Meanwhile, more intense summer rainfall may increase surface runoff and nutrient loading, heightening flood risks and degrading water quality.

ASSESSING AND UNDERSTANDING SPATIOTEMPORAL VARIATION IN
STABLE HYDROGEN AND OXYGEN ISOTOPE VALUES OF MARYLAND'S
RIVERS AND STREAMS

by

Syeda Sadia Ali

Thesis submitted to the Faculty of the Graduate School of the
University of Maryland, College Park, in partial fulfillment
of the requirements for the degree of
Master of Science
2025

Advisory Committee:

Professor Lee W. Cooper, Chair

Professor David M. Nelson

Professor Keith N. Eshleman

© Copyright by

Syeda Sadia Ali

2025

Dedication

To my mother

I carry you with me always—everything I do is to make you proud.

Acknowledgements

I would first like to express my sincere gratitude to my advisor, Dr. Lee Cooper, for giving me this incredible opportunity to be part of this program. His immense support, patience, and encouragement throughout the past two years have been invaluable. He has always been supportive, offering guidance and opening doors for help and suggestions. The numerous opportunities he has provided—ranging from participating in an Arctic cruise to attending various conferences—have significantly contributed to my scientific knowledge and expertise. I would also like to extend my heartfelt thanks to Dr. Jackie Grebmeier. As an international student, I had to navigate many new experiences, and both Dr. Cooper and Dr. Grebmeier have been incredibly welcoming and helpful at every step. I will always be grateful to them for making my transition to a new country so smooth and comfortable.

Additionally, I want to express my appreciation to my other committee members, Dr. David Nelson and Dr. Keith Eshleman, for sharing their expertise and knowledge throughout this project and for their valuable time and supervision. I am grateful to Kristen Heyer and her team at the Maryland Department of Natural Resources (DNR) for collecting the samples used in this study. I also extend my thanks to Dr. Cédric Magen for his support with mass spectrometric analysis and also for his invaluable guidance. I also want to thank the Maryland Water Resources Research Center at the University of Maryland, College Park, for their financial support through the Water Resources Research Act via the US Geological Survey.

My time at CBL would not have been the same without the incredible people who were an integral part of my graduate journey. I am especially grateful to Anna Hildebrand, whose friendship and

unwavering support mean the world to me. I also want to thank Amir Azarnivand, Allison Dreiss, Nick Silverson, and Amy Griffin for their wonderful friendship and camaraderie.

Finally, I want to express my deepest gratitude to my family—my father and my brother. My educational journey would not have been possible without my brother’s guidance and support throughout my life. Last but certainly not least, to my wonderful husband, Makin, who has been my greatest support system and biggest cheerleader—thank you for always believing in me.

Contents

Dedication	ii
Acknowledgements	iii
1. Introduction	1
1.1 Stable Isotope Analysis	2
1.1.1 Introduction to stable isotopes	2
1.1.2. Isotope Fractionation	4
1.2. Global and Local Meteoric Water Lines	5
1.3. The Role of Water Isotopes in River Hydrology	6
1.4. Rationale of the study	8
1.5. Research Objectives	10
2. Methods	11
2.1. Physiographic and Climatic Setting	11
2.2. River and Stream Sampling Sites	13
2.3. Data Collection	17
2.4. Isotopic Measurement	20
2.5. Data Analyses	21
2.5.1 LMWL, RWL & lc-excess	21
2.5.2. Moisture Surplus & Precipitation weighted average	22
2.5.3. Isotopic Relationships with Environmental Variables	23
2.5.4. Hydrograph Separation and Baseflow Index (BFI)	23
3. Results and Interpretations	26
3.1. General Overview of Isotopic Pattern	26
3.2. Precipitation Isotopic Composition	29
3.2.1. Weighted averages	29
3.2.2. Seasonal variability of precipitation	30
3.3. Local Meteoric Water Line (LMWL)	35
3.4. lc-excess	43
3.5. Elevation Effect on Isotopic Composition	45
3.6. d-excess	47
3.7. Hydrograph Separation and BFI index	50
3.7.1 Baseflow Separation Across Physiographic Regions	50
3.7.2. Optimal Hydrograph Separation Using Isotopes	51
3.7.3. Comparison of BFImax and Isotope Composition	57

4. Discussion	60
5. Limitations and Future studies	66
6. Climate Change impact	67
7. Conclusion	69
References	71

List of figures

Figure 1. Map of physiographic provinces in Maryland. (Source: Reger & Cleaves, 2008).	11
Figure 2. Spatial distribution of the 22 non-tidal river monitoring stations across Maryland. (DNR 2023). This figure was modified using qgis (https://qgis.org/).....	19
Figure 3. Annual surplus-weighted and precipitation-weighted isotopic values ($\delta^2\text{H}$) for river and stream. Left to right, the streams are arranged roughly west to east in location	29
Figure 4. Seasonal distribution of $\delta^{18}\text{O}$ (top) and $\delta^2\text{H}$ (bottom) in modelled precipitation grouped by physiographic region. Ridge plots display monthly isotopic density distributions for each site, colored by season. Black circles represent seasonal mean isotope value	32
Figure 5. Local Meteoric Water Line (LMWL) with the modeled data (red), Global Meteoric Water Line (GMWL) (blue), and Observed Line with Bostic data (green).	35
Figure 6. Site-specific river water line (RWL) equations for each river location.	42
Figure 7. Relationship between elevation and annual average river $\delta^2\text{H}$ and $\delta^{18}\text{O}$ values	45
Figure 8. Seasonal variation of $\delta^{18}\text{O}$ and $\delta^2\text{H}$ river values with elevation.....	46
Figure 9. Mean and variability of deuterium excess (d-excess) across 22 river and stream stations in Maryland. Black dots represent the mean d-excess value at each station, blue bars show the standard deviation, and whiskers indicate the full range of observed values (minimum to maximum).....	48
Figure 10. Hydrograph separation of quickflow and baseflow for five stations based on their physiographic variation.....	56
Figure 11. Comparison of SepHydro-derived BFI and optimized BFI _{max} values across five selected watersheds.....	57
Figure 12. Comparison of SepHydro-derived BFI and optimized BFI _{max} values across five Maryland watersheds	59

List of Tables

Table 1 . Climate, watershed, and precipitation isotopic data for the 22 gauged rivers included in the study.....	14
Table 2. Spatial variability of $\delta^2\text{H}$ and $\delta^{18}\text{O}$ across study locations, showing mean, maximum, and minimum values along with watershed area (km^2).	27
Table 3. Seasonal comparison of modeled precipitation and stream and river water $\delta^2\text{H}$ and $\delta^{18}\text{O}$ values across physiographic regions.....	33
Table 4. Site-specific river water line (RWL) equations for each river location.....	37
Table 5. lc -excess values for river water across 22 study locations in Maryland.....	43
Table 6. Mean deuterium excess (d-excess) values for selected Maryland river and stream sites	49
Table 7. Comparison of Sephydro BFI and optimized BFI _{max} with station-specific root mean square error (RMSE) values.....	51

1. Introduction

Human-induced climate change is significantly influencing Earth's water resources through altered precipitation patterns, enhanced evaporation, and an intensified hydrological cycle (Douville et al., 2021). Observations since the early 20th century reveal a general rise in precipitation across many regions—particularly in the northern hemisphere—attributed to anthropogenic warming (Knutson & Zeng, 2018). Climate models consistently project an increase in the frequency and intensity of extreme precipitation events across diverse climatic zones (Groisman et al., 2001; Najjar et al., 2010; Walsh et al., 2014). Rising air temperatures—averaging global increases of over 1°C since the early 1900s—are altering watershed water balances by increasing evapotranspiration and modifying moisture recycling processes (IPCC, 2014; Runkle et al., 2022). These shifts pose significant challenges for water management, particularly in low-lying coastal regions susceptible to tropical cyclones, and can compound damage from flooding. Mountain regions, which store and release snowmelt over time, are also seeing reduced snowpack and earlier melting, reducing water availability during dry periods (Mote et al., 2005; Barnett et al., 2008). Meanwhile, arid and semi-arid regions face growing risks from prolonged droughts, flash flooding, and more variable streamflow, further impacting limited water resources (Seager et al., 2007; Cayan et al., 2010). These changes affect river flow, stream levels, and groundwater–surface water interactions, emphasizing the need to understand climate impacts at local and regional scales. Despite growing evidence of these trends, our understanding of how seasonal precipitation, drought frequency, and extreme weather events reshape flow regimes and water budgets—especially within distinct physiographic provinces—remains incomplete, highlighting the need for finer-resolution watershed studies (Boesch et al., 2023).

1.1 Stable Isotope Analysis

1.1.1 Introduction to stable isotopes

Stable isotopes of water, particularly oxygen-18 ($\delta^{18}\text{O}$) and deuterium ($\delta^2\text{H}$), are naturally occurring variants of the atoms in the water molecule that differ in mass but not significantly in chemical behavior. They have been utilized as natural tracers to provide information about the kinetic and equilibrium processes that affect the hydrological cycle. These isotopes undergo fractionation during phase changes such as evaporation and condensation, leading to measurable variations in their ratios across different components of the hydrological cycle (Clark & Fritz, 1997). The stable isotope ratios of oxygen and hydrogen in water offer valuable insights into hydrological processes and can be used to assess how these processes influence climate variability and respond to long-term environmental change (Dee et al., 2023). The study of isotopic compositions in precipitation, pioneered by Dansgaard (1964), revealed correlations with temperature, altitude, latitude, precipitation amount, distance from the coast, and seasonality.

Hydrogen occurs naturally as three isotopes: ^1H , ^2H (deuterium), and ^3H (tritium). Oxygen also has three stable isotopes: ^{16}O , ^{17}O , and ^{18}O . These isotopes occur in nature at different abundances: approximately 99.985% for ^1H , 0.015% for ^2H , and trace amounts for the radioactive ^3H ; and 99.759%, 0.037%, and 0.204% for ^{16}O , ^{17}O , and ^{18}O , respectively (Bowen, 1986; Harris, 2005). Water molecules with different isotopic compositions form naturally, with the most common being $^1\text{H}_2\ ^{16}\text{O}$, $^1\text{H}_2\text{H}^{16}\text{O}$, $^1\text{H}_2\ ^{18}\text{O}$, and $^1\text{H}^3\text{H}^{16}\text{O}$ (Araguas-Araguas et al., 1997; Singh & Kumar, 2005). Fractionation of water molecules during phase changes causes variations in $\delta^2\text{H}$ and $\delta^{18}\text{O}$

composition, which are influenced by the mass differences of the isotopes (Kendall & Caldwell, 1998).

The stable isotopic composition of oxygen and hydrogen is given as a delta (δ) value for each isotope. The δ value in per mil (‰) can be given by:

$$\delta = (R_{\text{sample}} / R_{\text{standard}} - 1)1000] \quad (1)$$

Where,

R is the ratio of the heavy to light isotope

R_{sample} = sample of element of interest

R_{standard} = international reference standard of known composition, by convention set to zero

A positive value of δ , calculated by equation, indicates the enrichment of heavy isotopes compared to the established standard. A negative value of δ indicates the depletion of the heavy isotope compared to the established standard. The standard used for the stable water isotope analysis is Vienna Standard Mean Ocean Water (VSMOW), distributed internationally by the International Atomic Energy Agency. It is a laboratory-prepared standard that reflects the average isotopic composition of deep ocean water globally (Rohling 2013).

1.1.2. Isotope Fractionation

Mass-dependent isotope fractionation arises due to differences in isotope mass, and can be distinguished as two main types: equilibrium and kinetic fractionation (Kendall & Caldwell, 1998). Equilibrium fractionation in water occurs in closed systems where phase changes such as evaporation, condensation, freezing and thawing lead to an isotopic equilibrium if the molecules are subject to reversible phase changes. For example, in water, equilibrium fractionation influences the distribution of oxygen and hydrogen isotopes during evaporation and condensation within a boundary layer where phase changes are reversible (Sodemann, 2006). Since heavier isotopes (e.g., ^{18}O) diffuse more slowly and form stronger bonds than lighter isotopes (e.g., ^{16}O), evaporation preferentially removes lighter isotopes, leaving behind a water body enriched in the heavier isotopes. Conversely, condensation favors heavier isotopes, leading to a progressive depletion of ^{18}O in water vapor as it moves inland (Sodemann 2006).

Rayleigh distillation describes progressive isotope fractionation during phase changes, such as condensation during atmospheric moisture transport. As moist air cools and condenses, heavier isotopes (e.g., ^{18}O) are preferentially removed, leaving the remaining vapor increasingly depleted—a process mathematically captured by the Rayleigh equation (Clark & Fritz, 1997). In contrast, when moisture is moved toward warmer regions, evaporation and atmospheric recycling can dominate, leading to heavy isotopic enrichment as lighter isotopes are preferentially lost to the vapor phase (Gat, 1996; Sodemann, 2006). Rayleigh distillation gives a reasonable approximation of stable isotope behavior as fractionation occurs (Antunes et al., 2019).

Kinetic fractionation occurs when evaporation from a water source is not reversible and is influenced by external factors such as wind, and humidity. For example, lower humidity increases the irreversible loss of molecules passing through a boundary layer from a liquid water source into a vapor reservoir, while at higher humidity, there is a higher chance for molecules to return to the liquid source reservoir (Craig & Gordon, 1965).

1.2. Global and Local Meteoric Water Lines

This isotopic fractionation is expressed differently by oxygen and hydrogen atoms resulting in deviations from expected correlations between $^{18}\text{O}/^{16}\text{O}$ and $^2\text{H}/^1\text{H}$ isotope ratios in natural waters first described by Craig (1961) (equation 2), where $\delta^2\text{H}$ can be reasonably predicted for most waters as equaling.

$$8*\delta^{18}\text{O} + 10 \quad (2)$$

representing a global meteoric water line (GMWL), relating the isotopic fractionation of hydrogen isotopes to that observed for oxygen. Deviations from this correlation and regression line are termed deuterium excess (d-excess) (Dansgaard, 1964). which is defined as:

$$d=\delta^2\text{H}-8\delta^{18}\text{O} \quad (3)$$

It can directly reflect the degree of evaporation enrichment and the origin of water contributing to watershed recharge, such as precipitation, groundwater, or inflow from upstream sources (Brooks et al., 2012; Zhou et al., 2024). It can be used as a proxy for the humidity of the source region, with lower humidity associated with lower d values, so that the slope of 8 (equation 2) is reduced.

Alternately, deuterium excess values > 8 can indicate the presence of atmospheric vapor influenced by re-evaporation. Such elevated values have been observed in rivers across the Great Lakes region of the United States and Canada, as well as in other areas where evaporated moisture from lakes mixes with atmospheric water vapor (Machavaram & Krishnamurthy, 1995; Gat, 1996). This study examines whether "lake-effect" precipitation also extends into certain regions- from the western Appalachian highlands, central Piedmont to the eastern Coastal Plain of Maryland.

Local variations in climate, temperature, and evaporation lead to deviations from GMWL, forming Local Meteoric Water Lines (LMWLs) that better represent isotopic conditions in specific regions (Clark & Fritz 1997). The slope and intercept of LMWLs can vary significantly depending on local climatic factors (Gat 2010).

1.3. The Role of Water Isotopes in River Hydrology

Since the 1950s, stable isotope analysis has been applied to study global water cycling (e.g. Epstein & Mayeda, 1953; Dansgaard, 1964). However, its application in regional watershed studies did not become prevalent until the 1970s, with an early example being Dinçer et al. (1970). Their study used stable isotope techniques to evaluate the relative contributions of precipitation and groundwater to streamflow in small catchments. Over time, isotopic approaches have evolved into essential tools for evaluating watershed dynamics, providing insights into runoff generation, precipitation sources, groundwater-surface water interactions, water residence time, and evaporation effects (Gat, 1996; Bowen et al., 2019). Waters, such as lakes and rivers typically reflect the isotopic values of precipitation, which are correlated with important variables, including the seasonality of precipitation, temperature and elevation (e.g. Rozanski et al., 1993; Vachon et al., 2007; Henderson and Shuman, 2009). The main causes of variations in the stable-isotope

signature of river water are natural variations in the isotopic composition of rainfall, mixing with preexisting waters, and evaporation during percolation through soil and/or the unsaturated zone (Kendall and Caldwell, 1998).

The $\delta^{18}\text{O}$ and $\delta^2\text{H}$ values of precipitation are influenced by multiple environmental factors, including temperature, altitude, latitude, and isotopic values of the vapor source (reviewed by Kendall & Coplen, 2001). Temperature-driven fractionation during phase changes, along with how much of the original vapor remains after condensation and rainfall, strongly influence the isotope ratios in precipitation. Precipitation falling in coastal areas tends to have higher (less negative) $\delta^2\text{H}$ and $\delta^{18}\text{O}$ values because it usually has traveled a shorter distance from oceanic sources and has undergone less heavy isotope depletion (McGuire & McDonnell, 2007). Once precipitation falls within a watershed, its contribution to river discharge occurs through two primary pathways: delayed runoff (groundwater contributions) and direct runoff (overland flow) (McGuire & McDonnell, 2007). Direct runoff reaches rivers through surface pathways, direct precipitation onto the stream, and rapid shallow subsurface flow, with the relative contribution of these sources varying seasonally, geographically, and in response to human activities. These variations in runoff complicate the quantification of individual contributions to river discharge. Seasonal variation in river isotopic composition is generally more pronounced in rivers where recent precipitation is the primary source of flow, whereas it is more stable in streams dominated by groundwater inputs (Kendall & Coplen, 2001). The influence of evaporation on river water isotopes has also been well documented, particularly in warmer, low-elevation regions where evaporative enrichment of heavy isotopes is more pronounced (Simpson & Herczeg, 1991; Gremillion & Wanielist, 2000).

Topographic and climatic factors further influence the isotopic composition of river and stream water. River water in higher elevation regions typically shows lower $\delta^2\text{H}$ and $\delta^{18}\text{O}$ values,

reflecting input from precipitation that has undergone more rainout and experienced cooler temperatures (Rowley & Raymond, 2007). Similarly, seasonal differences in temperature and precipitation patterns usually result in river water having lower $\delta^2\text{H}$ and $\delta^{18}\text{O}$ values during the cool season compared to the warm season, as it reflects isotopically lighter precipitation inputs during colder months (Benettin et al., 2019).

1.4. Rationale of the study

Prior studies on the temporal and spatial variation of $\delta^2\text{H}$ and $\delta^{18}\text{O}$ values in river and stream water provide insights into regional water budgets (e.g., McGill et al., 2020; Halder et al., 2015; Gibson et al., 2002). In North America, research in the western United States has shown the dominance of winter snowmelt in annual stream water output at higher elevations, a pattern likely driven by low infiltration rates and high evapotranspiration during warmer months (Kendall & Coplen, 2001; Dutton et al., 2005). In contrast, studies of watersheds with significant lake and reservoir area in western North America suggest that precipitation from all seasons can contribute proportionally to water budgets, even during warm-season periods characterized by high moisture deficits (McGill et al., 2020). These differences between basins dominated by rivers versus those with large lakes or reservoirs areal extent likely reflect how moisture surpluses influence their respective annual water balances (Henderson & Shuman, 2009).

While studies on precipitation seasonality and isotopic variability in river recharge in eastern North America remain relatively limited, analyzing isotope fluctuations in surface runoff can provide valuable insights into regional hydrological processes. Establishing isotopic baselines has been recognized as a key tool for assessing hydrological processes in river systems (Reckerth et al., 2017). Additionally, isotopic studies in North America have demonstrated the ability to distinguish

between stormflow contributions and groundwater recharge in river systems, reinforcing the utility of stable isotope analysis for hydrological modeling (Burns et al., 2002; Gibson & Edwards, 2002; Rosa et al., 2016).

Maryland extends from upland mountainous areas (~1000 m elevation) to coastal lowlands over a relatively short geographic distance, making it a physiographically diverse region and an ideal setting for studying stable isotope variation in river and stream water. The state's varied terrain influences climate, hydrology, and water isotope composition, yet research on river-water isotopic variation in Maryland, to the best of my knowledge, remains scarce. Given the role that isotopic data play in understanding hydrological processes, my study aims to fill this gap by providing a baseline dataset for Maryland rivers and streams. This will enable future comparisons, improve predictions of hydrological responses to climate change, support water resource management strategies, and clarify the relative contributions of precipitation, groundwater, and evaporation to river flow in Maryland's surface water systems.

1.5. Research Objectives

The primary goal of this study is to establish a baseline isotopic dataset to support water resource management in Maryland and the greater mid-Atlantic region of the United States. This dataset can serve as a valuable reference for identifying hydrological processes influencing river systems and for assessing potential impacts of climate change on regional water resources—particularly in the context of shifting precipitation and runoff regimes.

The specific objectives of this study are:

- Evaluate Seasonal Precipitation Influence

Examine how seasonal precipitation patterns (cool-season vs. warm-season) influence the isotopic composition ($\delta^2\text{H}$ and $\delta^{18}\text{O}$) of river and stream water across Maryland.

- Assess Evaporation Effects Across Regions

Investigate the impact of evaporation on river water isotopic values and determine how these effects vary by location.

- Analyze Environmental Controls on Isotopic Composition

Identify the key hydrological, and physiographic variables (e.g., temperature, precipitation, elevation and relief, as well as watershed area) that control the spatial variability of river water isotope signals.

- Evaluate the Role of Lake-Effect Snow and Wetland Processes

Assess the influence of lake-effect precipitation and re-evaporation in wetlands on river-water isotopic composition.

2. Methods

2.1. Physiographic and Climatic Setting

Maryland spans a mountains-to-the-sea gradient and includes five major physiographic provinces: the Appalachian Plateau, the Ridge and Valley, the Blue Ridge, the Piedmont, and the Coastal Plain (Boward et al., 1999) (Figure 1). These regions exhibit distinct topographical and climatic characteristics that shape the state's hydrological systems. Elevations range from sea level in the Coastal Plain to a peak of approximately 1,025 m in the Appalachian Plateau of western Maryland (Backbone Mountain). Maryland contains a network of 14,164 km of freshwater streams and rivers (Boward et al., 1999), which play a major role in supporting ecosystems, providing water resources, and transporting freshwater to the Chesapeake Bay and other coastal estuaries.

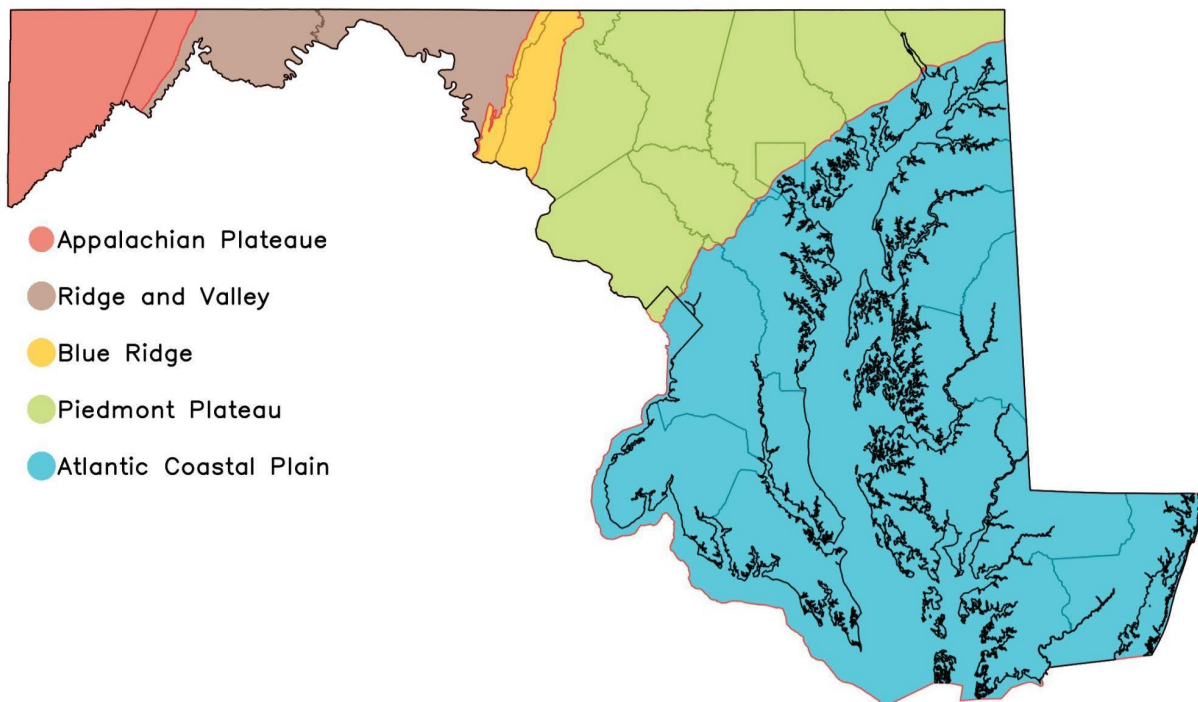


Figure 1. Map of physiographic provinces in Maryland. (Source: Reger & Cleaves, 2008).

According to the Köppen climate classification system, Maryland features a mix of humid subtropical and humid continental climates (Peel et al., 2007). Mean annual temperature (MAT) varies from 5°C in the Appalachian Plateau to 14°C in the eastern Coastal Plain. The Chesapeake Bay and Atlantic Ocean moderate temperatures in the eastern Coastal Plain, resulting in relatively mild winters and warm, humid summers. In contrast, western Maryland's higher elevations experience colder winters, greater seasonal temperature variation, and significant snowfall, occasionally influenced by lake-effect snow from the Great Lakes. The Piedmont and Ridge and Valley regions experience moderate climates, with rolling hills contributing to diverse hydrological conditions (Morgan & Cushman, 2005; Maryland DNR, 2005).

The sandy soils and shallow aquifers of the Coastal Plain allow for higher infiltration rates and support extensive wetlands and estuarine systems. Meanwhile, the more impermeable soils and steep terrain in the Piedmont and Appalachian regions promote higher surface runoff and more well-defined river networks (Cleaves et al., 1989). Mean annual precipitation (MAP) in Maryland varies across its physiographic provinces. For instance, Town Creek, located in Allegany County within the Ridge and Valley province, receives approximately 935 mm of precipitation annually. In contrast, Wheel Creek, situated in Harford County on the Coastal Plain, experiences an average annual precipitation of about 1,143 mm (Maryland State Climatologist Office). However, the hydrological effects of this precipitation vary due to physiographic and climatic factors such as elevation, topography, and groundwater interactions.

2.2. River and Stream Sampling Sites

This study used 22 non-tidal rivers and streams distributed across Maryland's physiographic provinces that represent the state's geographic and hydrological diversity (Table 1). The sites that were chosen take advantage of existing US Geological Survey (USGS) gauge infrastructure, and span a range of streams of varied watershed size, proximity to basin outlets, and accessibility during high-flow events (DNR, 2023). The watersheds sampled span a range of physiographic diversity. For example, Wills Creek flows through steep, high-elevation terrain, while central Maryland sites such as the Monocacy River lies within the rolling uplands of the Piedmont physiographic province, while Antietam Creek originates in the Ridge and Valley province and flows southwestward, crossing into the Blue Ridge before reaching the Piedmont. Eastern Coastal Plain streams, including Manokin Branch and Tuckahoe Creek, drain low-relief terrain with shallow aquifers and high wetland areal extent. It was expected that the diversity of climate, topography, and land cover would strongly influence the isotopic composition of surface waters through variations in precipitation-runoff relationships, groundwater recharge, and evaporative enrichment.

Table 1 . Climate, watershed, and precipitation isotopic data for the 22 gauged rivers included in the study.

Stream Name	Latitude (°N)	Longitude (°W)	MAP (mm)	MAT (°C)	Elevation (m) for sampling	Watershed Area (km ²)	Wetlands (%)	Physiographic Province (%)				
								CP	Pied	AP	VR	BR
Georges Creek	39.493	-79.044	1092.2	9.3	292	187.5	0	0	0	100	0	0
Wills Creek	39.669	-78.788	1051.6	5.2	336.5	639.73	0	0	0	81	19	0
Town Creek	39.553	-78.555	983	10.6	166.73	383.32	0	0	0	0	100	0
Sideling Hill Creek	39.649	-78.344	980.4	10.7	155.45	264.18	0	0	0	0	100	0
Tonoloway Creek	39.706	-78.152	988.1	10.8	121.62	287.49	0	0	0	0	100	0
Licking Creek	39.676	-78.042	1033.8	10.7	121.92	499.87	0	0	0	0	100	0
Antietam Creek Upstream	39.716	-77.606	1038.9	11.6	94.49	727.79	1	0	0	0	77	23

Antietam Creek Downstream	39.449	-77.73	1089.7	11.1	163.37	242.16	1	0	0	0	45	55
Catoctin Creek	39.427	-77.556	1112.5	11.7	114.3	173.27	0	0	4	0	10	86
Monocacy River	39.679	-77.235	1084.6	11.4	103.63	448.07	3	0	69	0	0	31
Patuxent River	39.238	-77.055	1122.7	12.3	110.95	90.13	3	0	100	0	0	0
Anacostia River	38.948	-76.956	1092.2	13.1	4.88	127.95	1	8	92	0	0	0
North Branch Patapsco River	39.503	-76.884	1117.6	12.1	128.02	146.59	1	0	100	0	0	0
Little Patuxent	39.167	-76.851	1125.2	12.8	78.94	98.42	7	0	100	0	0	0
Western Branch	38.814	-76.749	1079.5	13.3	127.1	232.32	4	100	0	0	0	0
Gwynns Falls	39.346	-76.733	1135.4	12.5	91.74	84.17	0	0	100	0	0	0
Wheel Creek	39.481	-76.34	1206.5	13.2	36.88	1.71	0	0	100	0	0	0
Deer Creek	39.617	-76.191	1168.4	12.1	14.33	424.76	1	0	100	0	0	0

Morgan Creek	39.28	-76.015	1110	13.1	3.87	32.89	6	100	0	0	0	0
Tuckahoe Creek	38.966	-75.943	1104.9	13.4	3.05	220.67	20	100	0	0	0	0
Big Elk Creek	39.667	-75.825	1178.6	11.7	25.3	136.23	1	0	100	0	0	0
Manokin Branch	38.213	-75.671	1102.4	13.9	1.83	12.43	46	100	0	0	0	0

MAP = Mean Annual Precipitation, MAT = Mean Annual Temperature, WS = watershed, CP = Coastal Plain, Pied = Piedmont, AP =

Appalachian Plateau, VR = Valley and Ridge, BR = Blue Ridge

2.3. Data Collection

The Maryland Department of Natural Resources (DNR) collects samples from fixed stations (Table 1) throughout the state as part of their non-tidal network for monitoring long-term changes in surface water quality (Maryland Department of Natural Resources, 2019) (Figure 2). DNR personnel collected one water sample per month at each site, regardless of hydrological conditions. These were typically baseflow samples, although some samples were taken during higher flow conditions, capturing a mix of groundwater and direct storm runoff. Additionally, eight storm-event samples per year were specifically collected at each site during high-flow conditions. When high discharge occurred during routine monthly sampling, samples were collected on the scheduled date using procedures for storm event sampling. In total, 20 samples were collected per site annually. Sampling was conducted from June 2022 to June 2024. The data obtained permitted the calculation of annual discharge-weighted isotope values at each site by integrating monthly isotope measurements with corresponding stream discharge data (U.S. Geological Survey, 2025). Specifically, the isotope values ($\delta^2\text{H}$ and $\delta^{18}\text{O}$) for each month were multiplied by that month's average discharge, summed across the year, and then divided by the total annual discharge to produce a discharge-weighted mean.

Depth-integrated water samples were collected from the middle of each river and stream using either an isokinetic sampler or a weighted bottle sampler with the isokinetic sampler being used if the centroid flow velocity exceeded 0.457 m/s. Depth integrated samples are composited (i.e., combined for each width interval in a churn sample splitter; DNR 2023). A sub-sample was transferred into a 20 mL scintillation bottle with a sealing conical polyethylene cap, which was further sealed with parafilm to prevent post-sampling evaporation.

Monthly precipitation data were obtained from county-level records provided by NOAA, while evaporation estimates were sourced from the Northeast Regional Climate Center (NRCC) at Cornell University, which offers gridded monthly evaporation datasets based on regional climate models. Daily stream discharge data for each river and stream were obtained from USGS stream gauge stations (U.S. Geological Survey, 2025).

The stable isotope values for precipitation used in this study were obtained using the Online Isotopes in Precipitation Calculator (OIPC), which provides modeled estimates rather than direct isotopic measurements at each location. These estimates are derived from the Global Network for Isotopes in Precipitation (GNIP), a database of observed $\delta^2\text{H}$ and $\delta^{18}\text{O}$ values compiled by the International Atomic Energy Agency and the World Meteorological Organization. Because many regions, including parts of Maryland, lack dense observational coverage, the OIPC employs a spatial interpolation model to generate site-specific isotope estimates (Bowen & Wilkinson, 2002; Bowen & Revenaugh, 2003; Bowen et al., 2005). The model incorporates geographic and climatic predictors such as latitude, longitude, elevation, distance from the coast, mean annual temperature, and precipitation to estimate both mean annual and monthly isotope values. The reliability of these modeled data is reflected in the 95% confidence intervals provided for each estimate, which quantify the statistical uncertainty based on spatial interpolation and residual variance from the underlying GNIP dataset. In order to help verify this interpolation-based estimate with real-world data, I compared the interpolated LMWL with a small set of measured precipitation isotope data provided by Dr. Joel Bostic (Garrett College, McHenry, Maryland, 21541, USA, unpublished data). The data included $\delta^{18}\text{O}$ and $\delta^2\text{H}$ values from individual rainfall events collected in 2018 and 2019 at Gunpowder Falls and Gwynn Falls.

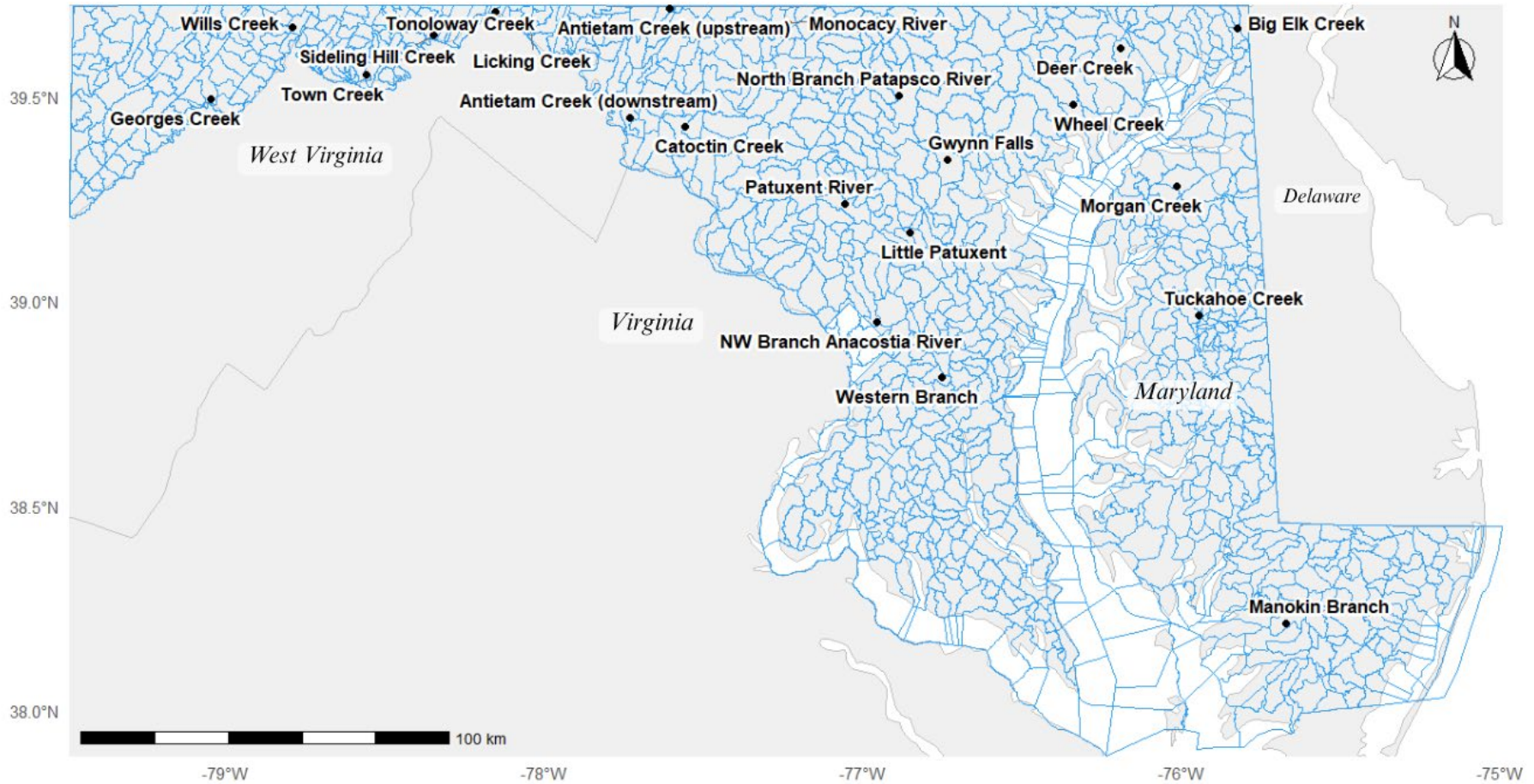


Figure 2. Spatial distribution of the 22 non-tidal river monitoring stations across Maryland. (DNR 2023). This figure was modified using qgis (<https://qgis.org/>).

2.4. Isotopic Measurement

Water samples were analyzed for stable isotope composition at the Chesapeake Biological Laboratory in Solomons, Maryland, using a ThermoFisher Gas Bench II peripheral coupled to a Delta V+ isotope ratio mass spectrometer (IRMS) operated in continuous-flow mode.

For $\delta^{18}\text{O}$ analysis, water samples were equilibrated with carbon dioxide (CO_2) in a helium- CO_2 mixture in airtight vials at a controlled temperature, allowing oxygen isotopes to exchange between the liquid water and gas phases. For $\delta^2\text{H}$, samples were placed in sealed vials with a platinum and copper catalyst, and a He- H_2 gas mixture was flushed through the vial to enable isotopic equilibration between the water and hydrogen gas generated from the gas cylinder. The equilibrated gas (CO_2 or H_2) was then introduced into the IRMS for $\delta^{18}\text{O}$ or $\delta^2\text{H}$ measurements, respectively. Hydrogen isotope measurements using IRMS are subject to interference from H_3^+ ion formation in the ion source, which affects the accuracy of the mass-to-charge (m/z) 3 signal. To correct for this, a H_3^+ correction factor was determined daily and applied, following standard procedures described by Coplen et al. (1991).

All isotope values are expressed in per mil (‰) relative to the Vienna Standard Mean Ocean Water (VSMOW). Analytical precision was $\pm 0.1\text{‰}$ for $\delta^{18}\text{O}$ and $\pm 1.0\text{‰}$ for $\delta^2\text{H}$, based on repeated measurements of internal laboratory standards calibrated to international reference materials. All $\delta^2\text{H}$ and $\delta^{18}\text{O}$ values were expressed using Equation 1 to express the ratios of heavy to light isotopes in the water sample relative to Vienna Standard Mean Ocean Water (VSMOW), respectively following normalization against two other standards, Standard Light Antarctic Precipitation (SLAP) and Greenland Ice Sheet Precipitation (GISP). Additionally, a separate quality control

standard, consisting of distilled water from Oak Ridge National Laboratory (ORNL), was used to monitor potential instrumental drift over time, ensuring consistent calibration accuracy and measurement precision.

2.5. Data Analyses

2.5.1 LMWL, RWL & lc-excess

The linear regression of the modeled monthly precipitation isotope data for the 22 stream sites, extracted from the OIPC, was used to predict the Local Meteoric Water Line (LMWL). This line was constructed from 264 values (12 monthly estimates per site) and captured the isotopic characteristics of precipitation inputs across Maryland's physiographic regions. While the OIPC estimates are spatially interpolated, their use in this study provides a standardized isotopic baseline across sites despite variability in basin elevation and geographic extent. River Water Lines (RWLs) were also evaluated for each site through linear regression of $\delta^2\text{H}$ against $\delta^{18}\text{O}$ values of the baseflow data. The intersection of the river water lines with the GWML or LMWL provide a river water input value that describes the subsequent isotopic behavior of water in each river or stream and identifies hydrologic processes such as precipitation input, evaporation, and groundwater mixing that modify isotopic content once within the stream or river.

The local meteoric water line excess (lc-excess) was also computed to identify river water samples that deviate from expected isotopic patterns due to meteorological influences. Specially, the lc-excess quantifies how far a sample lies from the Local Meteoric Water Line, offering insight into processes like evaporation or mixing (Landwehr and Coplen, 2006). The lc-excess was calculated using the equation:

$$\text{lc-excess} = (\delta^2\text{H} - a \times \delta^{18}\text{O} - b) / s \quad (4)$$

Where,

a and b are the slope and intercept of the LMWL and s is the standard error (uncertainty) of the regression.

2.5.2. Moisture Surplus & Precipitation weighted average

Two approaches were used to calculate the annual average isotopic values of the precipitation estimates. The first approach utilized moisture surplus-weighted averaging, which considered only those months in which precipitation exceeded evaporation. This method aimed to capture the isotopic composition of effective precipitation—that is, the portion contributing to groundwater recharge and streamflow—aligning with the methodology described by Peng et al. (2004).

Moisture surplus values were calculated monthly using the equation:

$$\text{Moisture Surplus} = P_1 - E_1 \quad (5)$$

Where,

P_1 is the precipitation and E_1 is the evaporation for designated month.

Only the months with positive moisture surplus were included in the moisture surplus-weighted isotopic calculations. The second approach applied a precipitation-weighted averaging, which included all months and weighted isotopic values by the total monthly precipitation, thereby capturing broader seasonal variations (Swenson et al., 2006).

2.5.3. Isotopic Relationships with Environmental Variables

Simple regression analyses were performed between $\delta^2\text{H}$ and $\delta^{18}\text{O}$ values and key environmental variables, including mean annual temperature (MAT), mean annual precipitation (MAP), elevation, and watershed area to explore hydrological, climatic, and physiographic controls on isotopic composition (Welch et al., 2017; McGill et al., 2020).

2.5.4. Hydrograph Separation and Baseflow Index (BFI)

Hydrograph separation is a hydrological technique used to distinguish between different sources of streamflow—typically separating baseflow (groundwater contribution) from stormflow (surface

runoff)— to better understand watershed response to precipitation events (Wels et al., 1991). Hydrologic flow contributions were examined using the web-based tool SepHydro (<https://sephydro.hydrotools.tech/pageMain.php>), which implements the Lyne and Hollick recursive digital filter method (Lyne & Hollick, 1979), with α -values informed by the Eckhardt digital filter approach (Danielescu, 2018). For each station, I uploaded daily streamflow data and computed the Baseflow Index (BFI), representing the proportion of total streamflow derived from groundwater (Antonia & Paolo, 2008). For the comparison study, I selected five representative stream sites from each of the five distinct physiographic regions across Maryland: Georges Creek (Appalachian Plateau), Town Creek (Valley and Ridge), Catoctin Creek (Blue Ridge), Patuxent River (Piedmont), and Western Branch (Coastal Plain).

To further assess the accuracy of this separation, I applied the Optimal Hydrograph Separation (OHS) technique, which uses isotopic tracer data ($\delta^2\text{H}$ and $\delta^{18}\text{O}$) to calibrate the BFI_{max} parameter in the filter, following the approach outlined by Foks et al. (2019). This method involved minimizing the root mean square error (RMSE) between observed stream $\delta^2\text{H}$ and $\delta^{18}\text{O}$ values and simulated isotope values derived from a recursive digital filter, using fixed baseflow and stormflow endmember compositions. These values were assigned based on the average isotope values of samples collected during baseflow and stormflow conditions at each site, respectively. Baseflow samples were identified with observations of sustained low-flow periods, while stormflow samples corresponded to rising limb or peak discharge following precipitation events. I then compared the SepHydro-derived annual average BFI values with the isotope-optimized BFI_{max} values, and visualized these alongside the annual mean $\delta^2\text{H}$ and $\delta^{18}\text{O}$ values (± 1 standard deviation) for each

station. All statistical analyses and visualizations were conducted in R version 4.2.2 using appropriate packages such as ggplot2, dplyr, and tidyr (<https://www.r-project.org/>).

3. Results and Interpretations

3.1. General Overview of Isotopic Pattern

The isotopic composition of river water samples across the study locations demonstrates significant spatial variability in both $\delta^2\text{H}$ and $\delta^{18}\text{O}$ values, consistent with meteoric water inputs and natural isotopic fractionation processes. The locations with the lowest weighted mean $\delta^2\text{H}$ and $\delta^{18}\text{O}$ values were the westernmost sites, Georges Creek ($\delta^2\text{H}$: -53‰ , $\delta^{18}\text{O}$: -8.5‰) and Wills Creek ($\delta^2\text{H}$: -51‰ , $\delta^{18}\text{O}$: -7.9‰). In contrast, less negative $\delta^2\text{H}$ and $\delta^{18}\text{O}$ values were recorded in southeastern sites, Manokin Branch ($\delta^2\text{H}$: -29‰ , $\delta^{18}\text{O}$: -5.7‰) and Western Branch ($\delta^2\text{H}$: -34‰ , $\delta^{18}\text{O}$: -6.0‰) (Table 2).

Table 2. Spatial variability of $\delta^2\text{H}$ and $\delta^{18}\text{O}$ across study locations, showing mean, maximum, and minimum values along with watershed area (km^2).

Location	Watershed Area (km^2) above sampling site	Mean		Maximum		Minimum	
		$\delta^2\text{H}$ (‰)	$\delta^{18}\text{O}$ (‰)	$\delta^2\text{H}$ (‰)	$\delta^{18}\text{O}$ (‰)	$\delta^2\text{H}$ (‰)	$\delta^{18}\text{O}$ (‰)
Georges Creek	187.5	-53	-8.5	-41	-7.4	-66	-10.3
Wills Creek	639.73	-51	-7.9	-34	-5.1	-62	-9.0
Town Creek	383.32	-47	-7.7	-38	-5.7	-56	-8.8
Sideling Hill Creek	264.18	-45	-7.1	-26	-3.1	-60	-9.4
Tonoloway Creek	287.49	-44	-7.3	-29	-5.3	-55	-8.9
Licking Creek	499.87	-46	-7.5	-30	-5.9	-66	-10.3
Antietam Creek upstream	727.79	-46	-7.7	-31	-5.8	-61	-9.4
Antietam Creek downstream	242.16	-46	-7.5	-29	-4.0	-65	-9.7
Catoctin Creek	173.27	-43	-7.4	-31	-5.5	-75	-11.3
Monocacy River	448.07	-39	-6.8	-21	-4.1	-58	-9.1
Patuxent River	90.13	-42	-7.0	-28	-2.3	-57	-9.2

NW Branch Anacostia River	127.95	-36	-6.1	-13	-2.9	-73	-10.7
North Branch Patapsco River	146.59	-38	-6.5	-18	-3.4	-60	-9.4
Western Branch (Patuxent River)	98.42	-34	-6.0	-11	-3.0	-66	-10.0
Gwynn Falls	232.32	-37	-6.6	-18	-4.1	-82	-12.6
Tuckahoe Creek	84.17	-34	-6.0	-13	-4.6	-43	-7.6
Big Elk Creek	1.71	-37	-6.6	-26	-5.1	-68	-9.3
Manokin Branch	424.76	-29	-5.7	-15	-3.6	-49	-8.5
Little Patuxent	32.89	-36	-6.2	-24	-3.8	-60	-9.4
Wheel Creek	220.67	-38	-6.6	-18	-4.8	-59	-12.0
Deer Creek	136.23	-41	-6.9	-35	-6.4	-54	-8.5
Morgan Creek	12.43	-34	-6.3	-23	-4.1	-46	-8.5

3.2. Precipitation Isotopic Composition

3.2.1. Weighted averages

Computed moisture surplus-weighted isotope values based on the OIPC interpolation model were consistently lower in 2023–2024 compared to 2022–2023 across the stations, with the largest differences observed at western sites like Georges Creek and Wills Creek (Figure 3). Precipitation-weighted $\delta^2\text{H}$ values were only marginally lower in 2023–2024. Across both years, surplus-weighted $\delta^2\text{H}$ values were only marginally lower in 2023–2024. Across both years, surplus-weighted $\delta^2\text{H}$ values were consistently lower than precipitation-weighted values, reflecting the presence of lighter isotopes from cold-season recharge. Western Maryland sites had the lowest values, consistent with greater winter precipitation input, while eastern sites showed higher values, suggesting more evaporation or influence from summer rainfall.

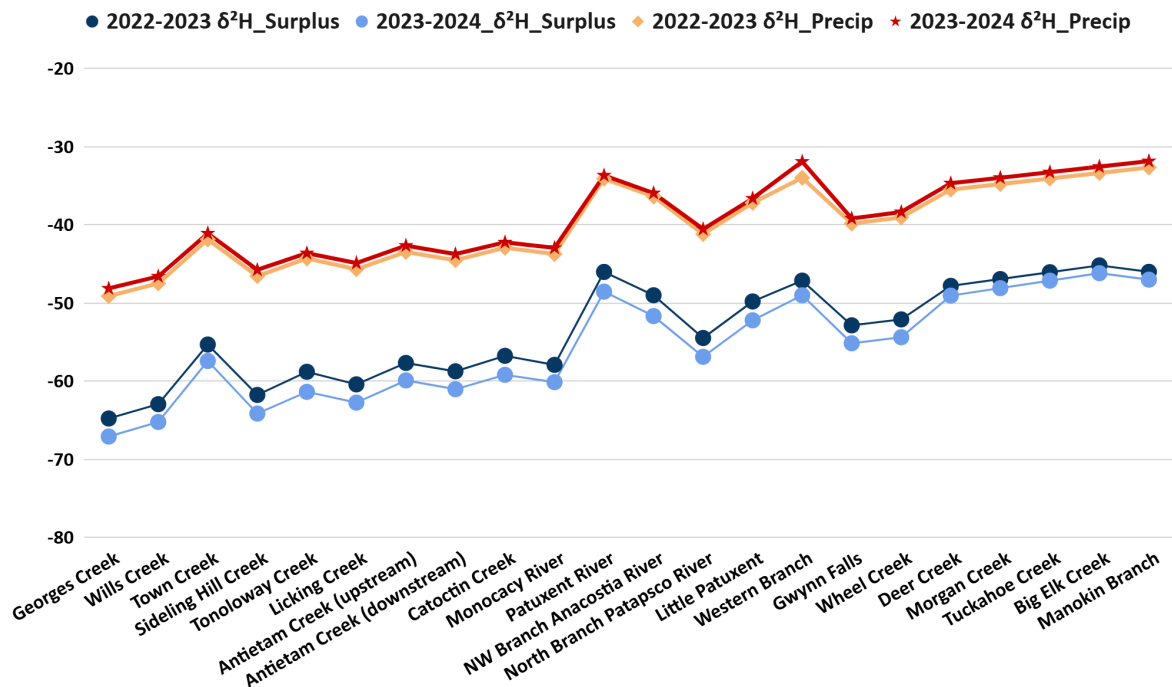
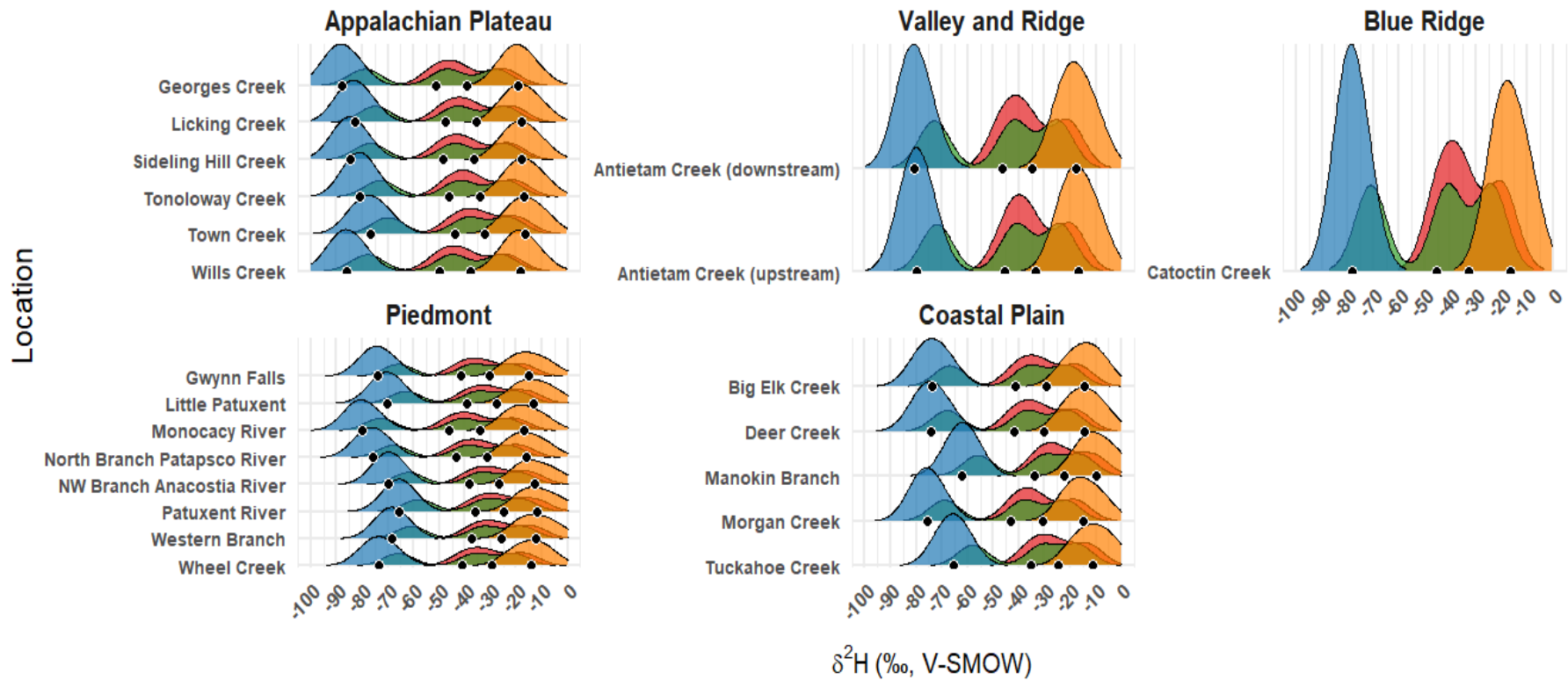


Figure 3. Annual surplus-weighted and precipitation-weighted isotopic values ($\delta^2\text{H}$) for river and stream. Left to right, the streams are arranged roughly west to east in location

3.2.2. Seasonal variability of precipitation

Both heavy isotopes (^{18}O and ^2H) in precipitation displayed distinct seasonal trends, with winter precipitation exhibiting the lowest isotopic values, and summer showing the highest values, consistent with seasonal temperature and moisture source effects (Figure 4).

When comparing modeled precipitation isotope values with measured river and stream water across Maryland's physiographic regions, a seasonal pattern was found. In all physiographic regions, river water was isotopically heavier than winter precipitation and lighter than summer precipitation based on both $\delta^2\text{H}$ and $\delta^{18}\text{O}$ values (Table 3).



Season ■ Fall (Sept–Nov) ■ Spring (Mar–May) ■ Summer (Jun–Aug) ■ Winter (Dec–Feb)

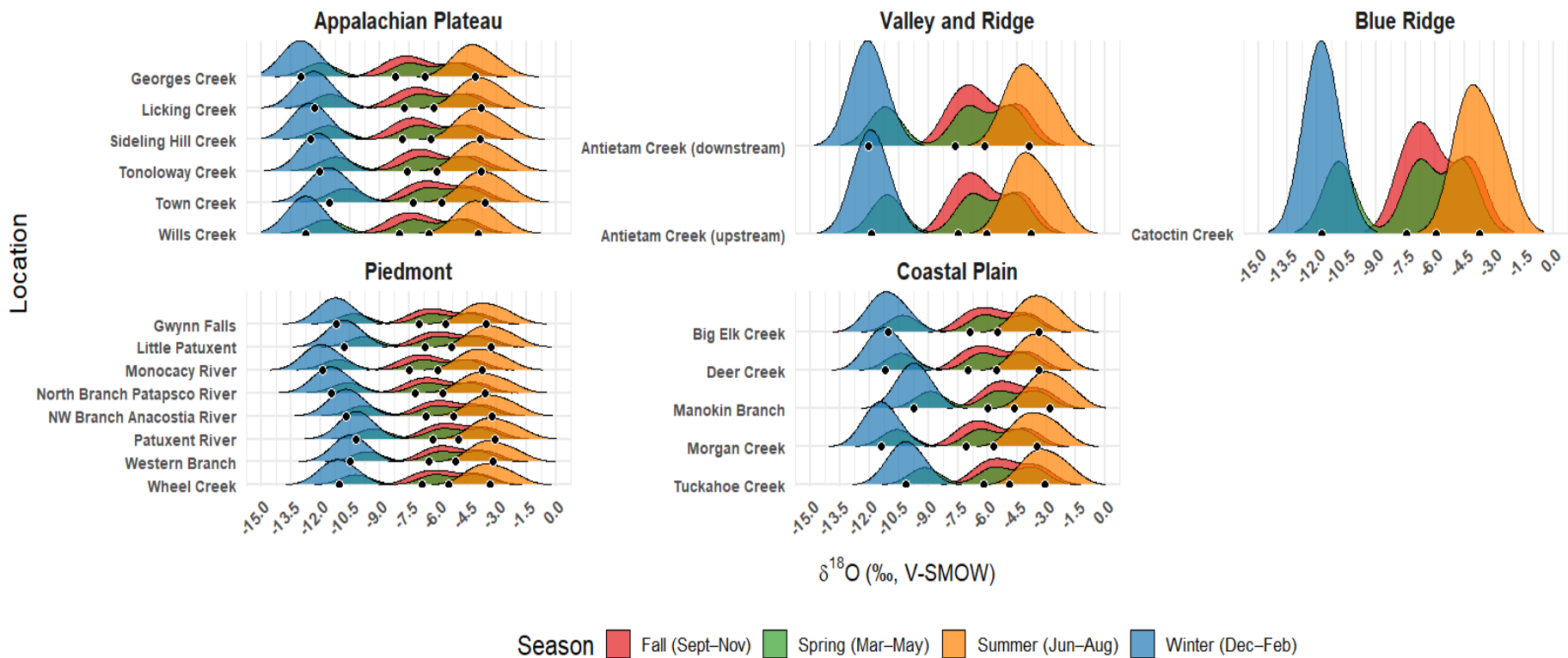


Figure 4. Seasonal distribution of $\delta^{18}\text{O}$ (top) and $\delta^2\text{H}$ (bottom) in modelled precipitation grouped by physiographic region. Ridge plots display monthly isotopic density distributions for each site, colored by season. Black circles represent seasonal mean isotope value

Table 3. Seasonal comparison of modeled precipitation and stream and river water $\delta^2\text{H}$ and $\delta^{18}\text{O}$ values across physiographic regions

Season	Isotope	Region	Mean River Isotope (‰)	Mean Modeled Precip Isotope (‰)
Fall (Sept–Nov)	$\delta^2\text{H}$	Appalachian Plateau	-43.2	-42.8
	$\delta^{18}\text{O}$	Appalachian Plateau	-7.3	-7.2
	$\delta^2\text{H}$	Ridge and Valley	-39.1	-39.5
	$\delta^{18}\text{O}$	Ridge and Valley	-6.9	-6.8
	$\delta^2\text{H}$	Coastal Plain	-34.8	-33.5
	$\delta^{18}\text{O}$	Coastal Plain	-6.2	-6
	$\delta^2\text{H}$	Piedmont	-34.4	-35.4
	$\delta^{18}\text{O}$	Piedmont	-6.2	-6.3
Spring (Mar–May)	$\delta^2\text{H}$	Appalachian Plateau	-50.9	-47.9
	$\delta^{18}\text{O}$	Appalachian Plateau	-7.9	-7.8
	$\delta^2\text{H}$	Ridge and Valley	-43.2	-45.3
	$\delta^{18}\text{O}$	Ridge and Valley	-7.4	-7.4
	$\delta^2\text{H}$	Coastal Plain	-36.8	-39.1
	$\delta^{18}\text{O}$	Coastal Plain	-6.4	-6.6
	$\delta^2\text{H}$	Piedmont	-37.6	-41

	$\delta^{18}\text{O}$	Piedmont	-6.5	-6.9
Summer (Jun–Aug)	$\delta^2\text{H}$	Appalachian Plateau	-44.5	-17.8
	$\delta^{18}\text{O}$	Appalachian Plateau	-6.8	-3.9
	$\delta^2\text{H}$	Ridge and Valley	-38.5	-16.7
	$\delta^{18}\text{O}$	Ridge and Valley	-6.6	-3.8
	$\delta^2\text{H}$	Coastal Plain	-34	-13
	$\delta^{18}\text{O}$	Coastal Plain	-5.8	-3.2
	$\delta^2\text{H}$	Piedmont	-33.3	-14.4
	$\delta^{18}\text{O}$	Piedmont	-5.5	-3.5
Winter (Dec–Feb)	$\delta^2\text{H}$	Appalachian Plateau	-52.7	-85.8
	$\delta^{18}\text{O}$	Appalachian Plateau	-8.5	-12.7
	$\delta^2\text{H}$	Ridge and Valley	-52.2	-80.5
	$\delta^{18}\text{O}$	Ridge and Valley	-8.3	-12.1
	$\delta^2\text{H}$	Coastal Plain	-35.1	-72.7
	$\delta^{18}\text{O}$	Coastal Plain	-6.8	-11
	$\delta^2\text{H}$	Piedmont	-44.2	-75.4
	$\delta^{18}\text{O}$	Piedmont	-7.6	-11.4

3.3. Local Meteoric Water Line (LMWL)

The regional LMWL from the calculated average monthly $\delta^2\text{H}$ and $\delta^{18}\text{O}$ values of precipitation based on the OIPC model for each watershed is (Figure 5):

$$\delta^2\text{H} = 7.84 \cdot \delta^{18}\text{O} + 12.86 \quad (R^2 = 0.99)$$

The linear regression of the unpublished precipitation data from Joel Bostic produced a line with a slope of 7.38 and an intercept of 16.25, which is similar to the Interpolated LMWL and supports its validity as a baseline for local meteoric input in this study.

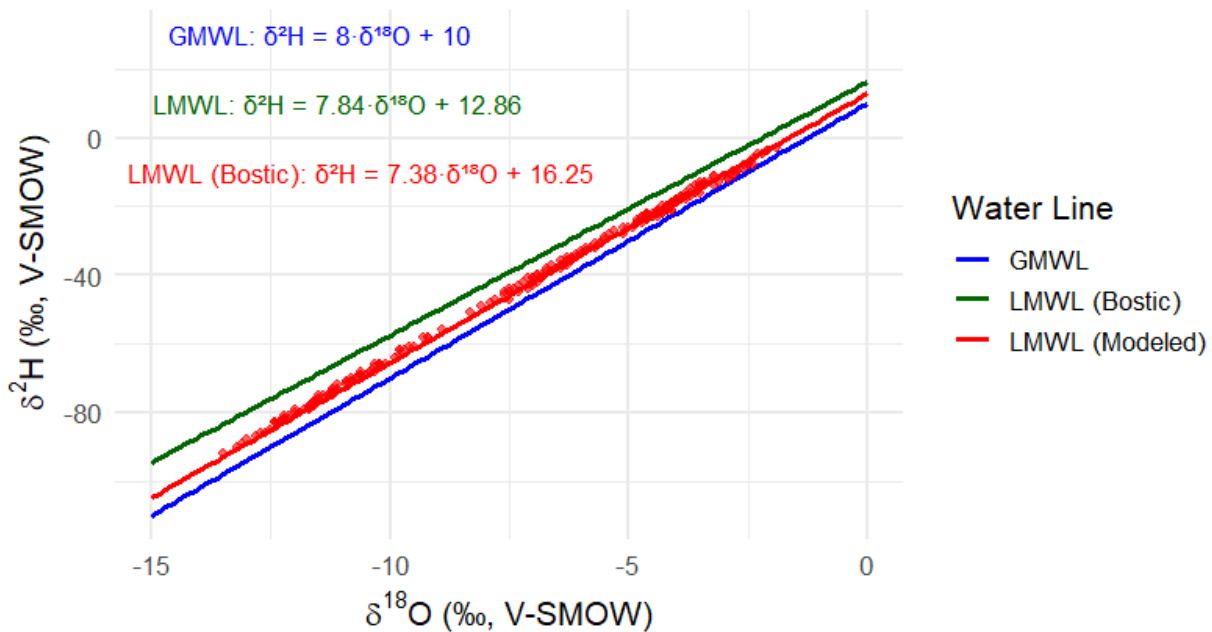


Figure 5. Local Meteoric Water Line (LMWL) with the modeled data (red), Global Meteoric Water Line (GMWL) (blue), and Observed Line with Bostic data (green).

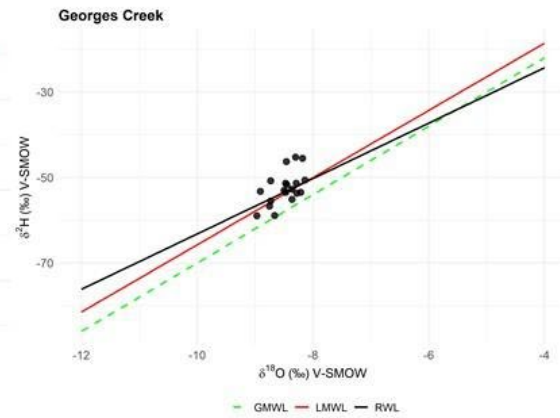
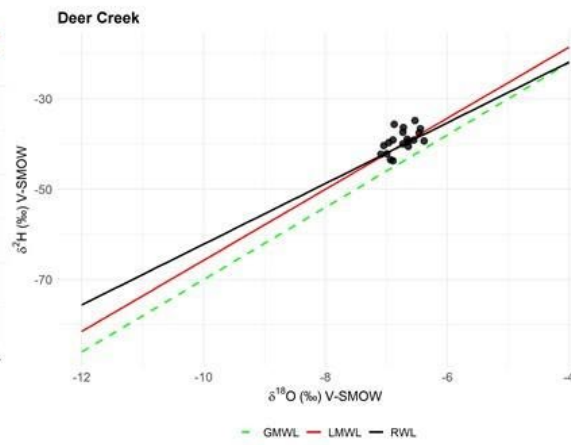
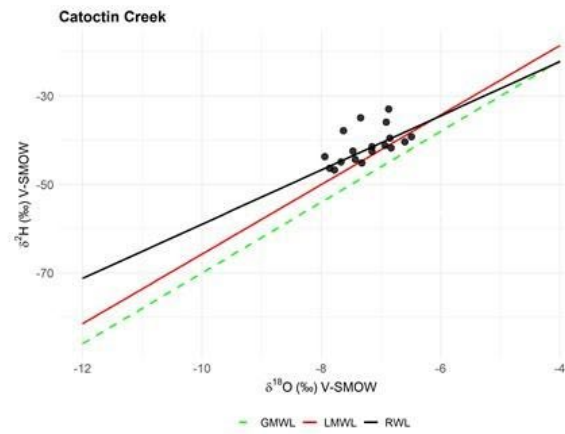
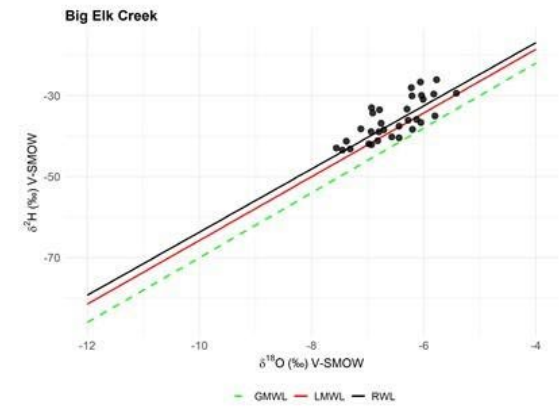
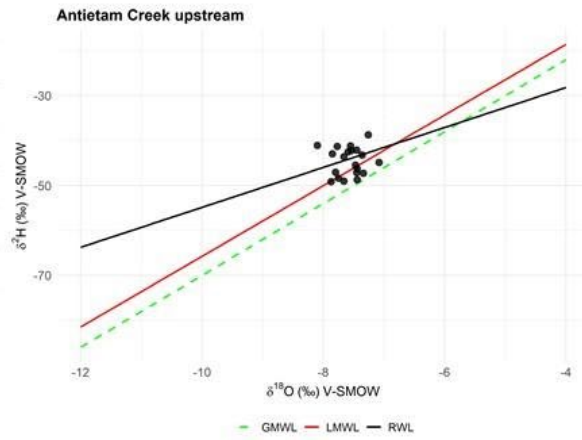
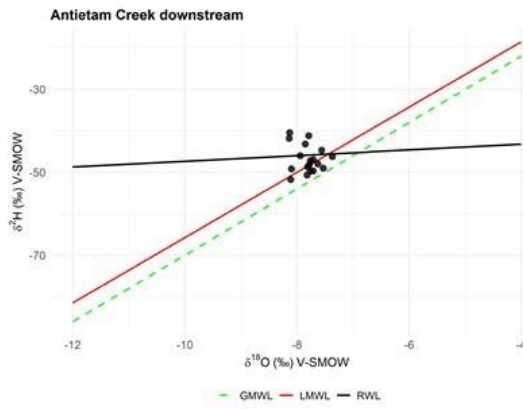
River Water Line (RWL) slopes varied widely across sites, highlighting differences in evaporation, source water contributions, and hydrologic settings (Figure 6; Table 4). Sites with comparatively high-relief watersheds such as Georges Creek, Deer Creek, and Catoctin Creek showed slopes that closely paralleled the Local Meteoric Water Line (LMWL), indicating minimal evaporation and a strong, unaltered meteoric signal. In contrast, flatter sites—including Antietam Creek (Downstream), Morgan Creek, and Western Branch—exhibited shallower RWL slopes, suggesting greater evaporative effect or more mixing with surface runoff. On the Eastern Shore, sites such as Manokin Branch and Big Elk Creek clustered above the LMWL but with slightly flatter slopes, consistent with higher temperatures and evaporation effects.

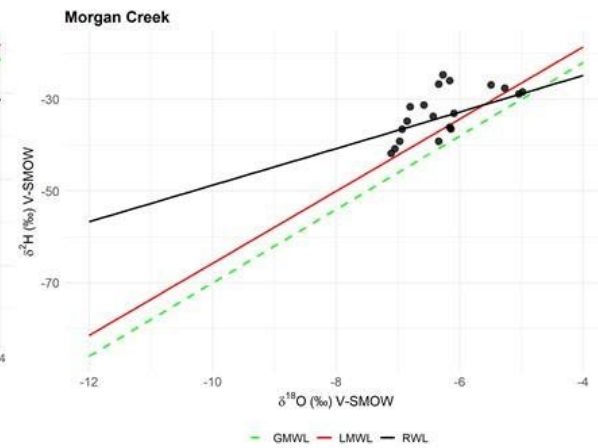
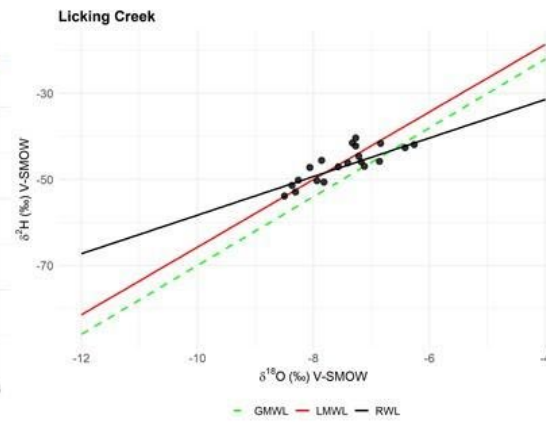
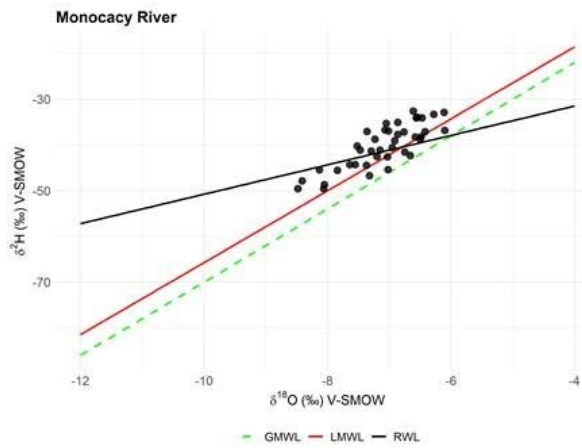
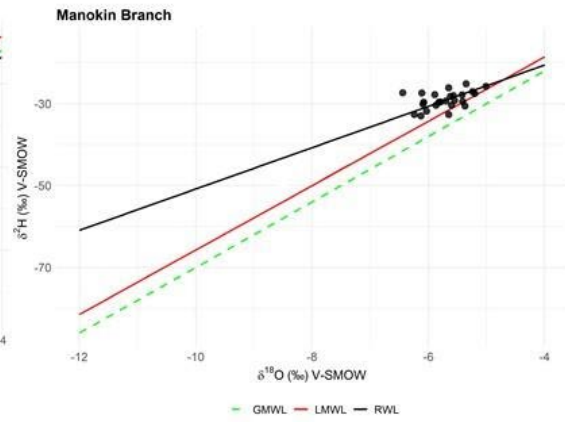
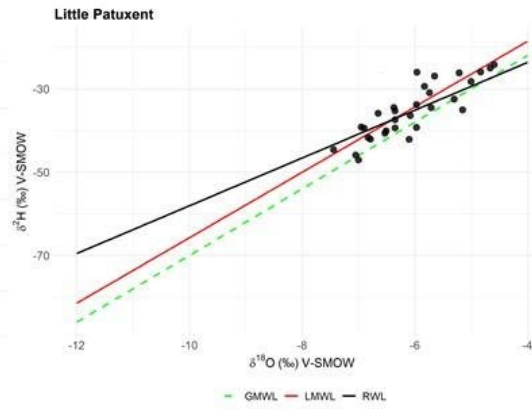
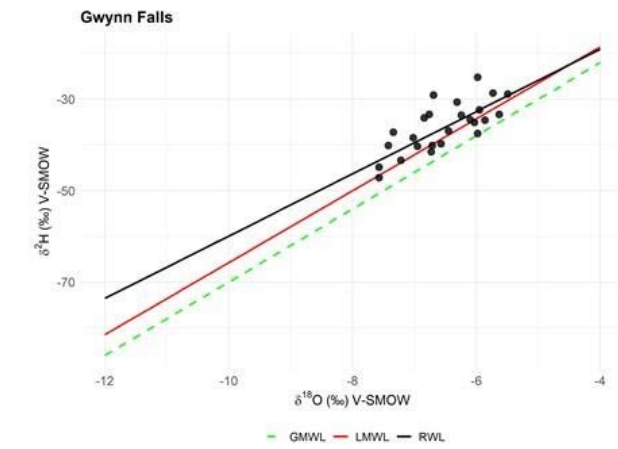
At some sites, particularly Antietam Creek Downstream and Deer Creek, the isotopic spread was limited, and the regression showed a poor fit (low R^2 values). However, since we are only considering baseflow isotope values for the sites, the small range in isotope values is likely expected because groundwater tends to stay stable over time. RWLs were fitted using simple linear regression without outlier removal; slight misfits at some sites might reflect the influence of sample size and natural variability.

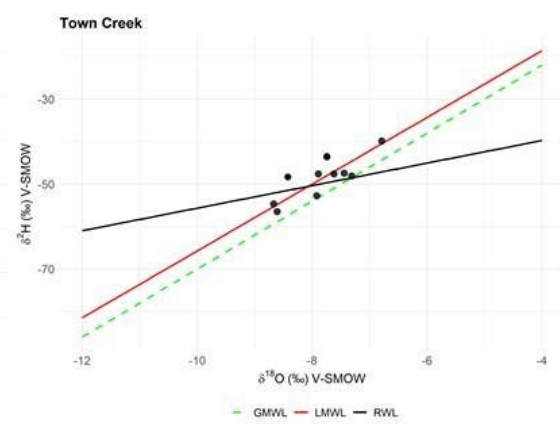
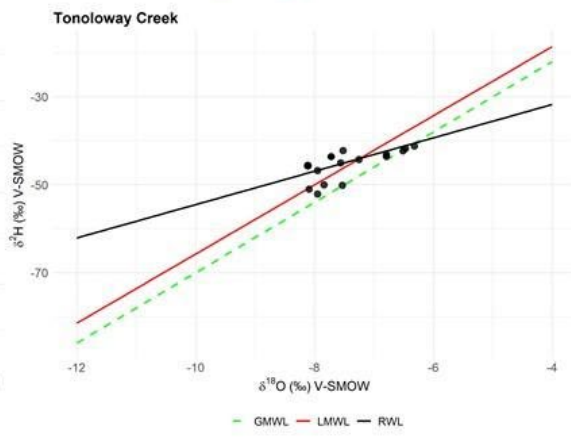
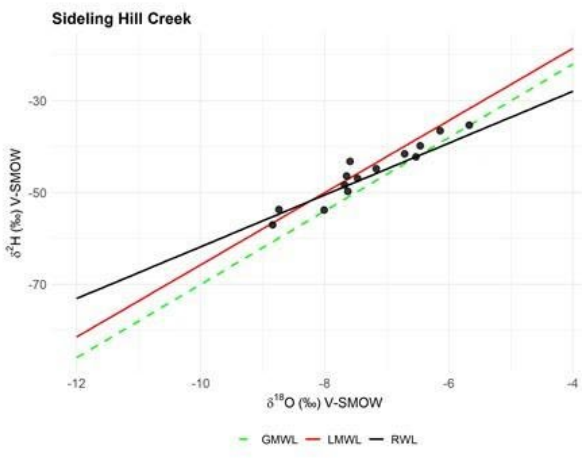
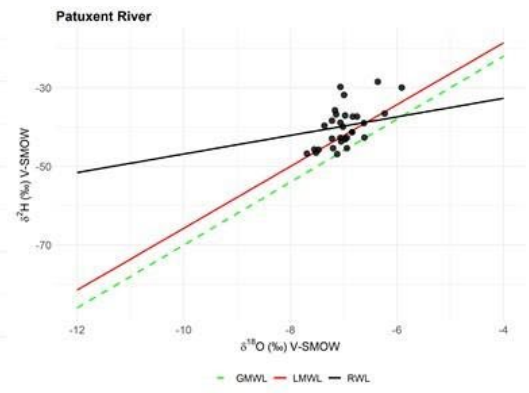
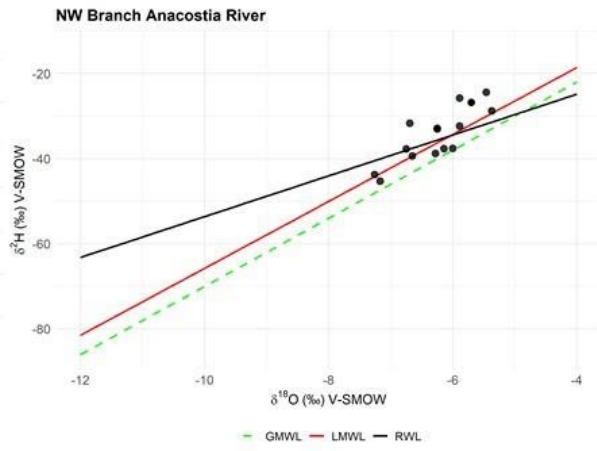
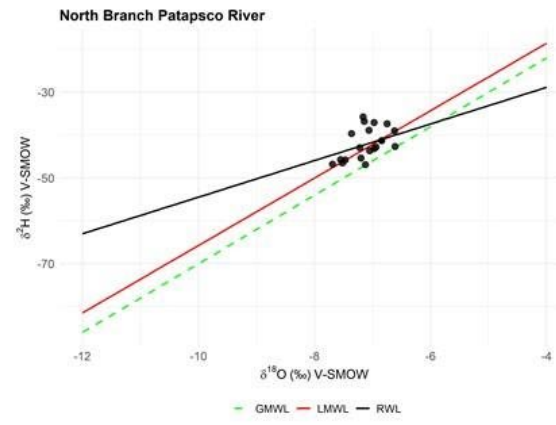
Table 4. Site-specific river water line (RWL) equations for each river location

Location	Equation	Standard error of the slope
Georges Creek	$\delta^2\text{H} = 6.92 \delta^{18}\text{O} + 5.95$	0.18
Wills Creek	$\delta^2\text{H} = 2.15 \delta^{18}\text{O} + (-33.96)$	0.18
Town Creek	$\delta^2\text{H} = 3.8 \delta^{18}\text{O} + (-18.13)$	0.24
Sideling Hill Creek	$\delta^2\text{H} = 5.77 \delta^{18}\text{O} + (-4)$	0.15
Tonoloway Creek	$\delta^2\text{H} = 4.26 \delta^{18}\text{O} + (-13.38)$	0.19
Licking Creek	$\delta^2\text{H} = 6.44 \delta^{18}\text{O} + 2.19$	0.27
Antietam Creek (upstream)	$\delta^2\text{H} = 5.02 \delta^{18}\text{O} + (-7.3)$	0.19
Antietam Creek (downstream)	$\delta^2\text{H} = 2.8 \delta^{18}\text{O} + (-24.98)$	0.21
Catoctin Creek	$\delta^2\text{H} = 7.04 \delta^{18}\text{O} + 8.82$	0.27
Monocacy River	$\delta^2\text{H} = 6 \delta^{18}\text{O} + 1.48$	0.29

Patuxent River	$\delta^2\text{H} = 2.37 \delta^{18}\text{O} + (-8.73)$	0.27
NW Branch Anacostia River	$\delta^2\text{H} = 6.63 \delta^{18}\text{O} + 4.97$	0.16
North Branch Patapsco River	$\delta^2\text{H} = 4.25 \delta^{18}\text{O} + (-10.13)$	0.21
Little Patuxent River	$\delta^2\text{H} = 5.73 \delta^{18}\text{O} + (-0.72)$	0.34
Western Branch of Patuxent River	$\delta^2\text{H} = 5.57 \delta^{18}\text{O} + 8.82$	0.32
Gwynn Falls	$\delta^2\text{H} = 6.59 \delta^{18}\text{O} + 6.13$	0.32
Wheel Creek	$\delta^2\text{H} = 7.27 \delta^{18}\text{O} + 10.14$	0.34
Deer Creek	$\delta^2\text{H} = 6.71 \delta^{18}\text{O} + (-8.87)$	0.18
Morgan Creek	$\delta^2\text{H} = 3.98 \delta^{18}\text{O} + (-8.87)$	0.26
Tuckahoe Creek	$\delta^2\text{H} = 5.46 \delta^{18}\text{O} + (-0.92)$	0.19
Big Elk Creek	$\delta^2\text{H} = 7.79 \delta^{18}\text{O} + 14.23$	0.22
Manokin Branch	$\delta^2\text{H} = 7.13 \delta^{18}\text{O} + (-25.1)$	0.3







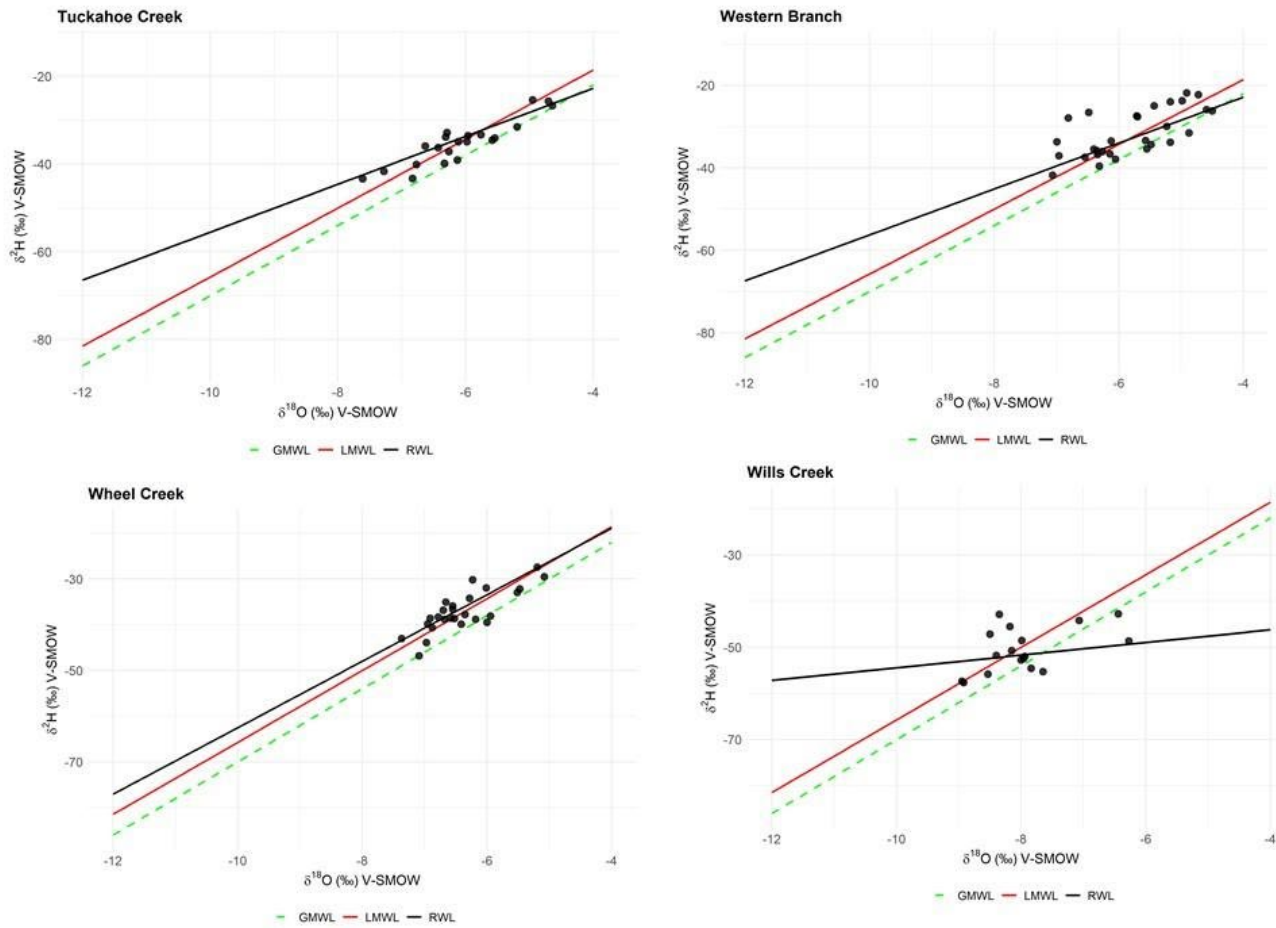


Figure 6. Site-specific river water line (RWL) equations for each river location.

3.4. *lc-excess*

Line-conditioned excess (*lc-excess*) was calculated for each stream and river station to evaluate deviations of individual water samples from the site-specific RWL (Table 5). Spatial patterns in *lc-excess* varied across the 22 study sites, reflecting differences in hydrological inputs and surface–subsurface interactions. Higher *lc-excess* values—indicating minimal deviation from the RWL—were observed at stations such as Manokin Branch, Morgan Creek, and Gwynn Falls, suggesting that streamflow at these sites was primarily derived from recent precipitation with limited evaporation or isotopic fractionation. These sites likely receive substantial contributions from shallow or rapidly transmitted runoff with little time for isotopic alteration. In contrast, more negative *lc-excess* values were recorded at Sideling Hill Creek, Wills Creek, and Little Patuxent River, indicating that the water at these locations had undergone greater isotopic modification. This could result from evaporation during overland flow, interaction with older or more isotopically fractionated groundwater, or prolonged surface exposure.

Table 5. lc-excess values for river water across 22 study locations in Maryland

Location	lc-excess
Sideling Hill Creek	-2.13
Wills Creek	-1.88
Little Patuxent	-0.55
NW Branch Anacostia River	-0.34
Tonoloway Creek	-0.05

Licking Creek	0.03
Deer Creek	0.04
Antietam Creek upstream	0.13
Town Creek	0.25
Patuxent River	0.27
Western Branch	0.27
Tuckahoe Creek	0.59
Georges Creek	1.03
Monocacy River	1.17
Wheel Creek	1.18
North Branch Patapsco River	1.63
Antietam Creek downstream	1.81
Big Elk Creek	1.82
Catoctin Creek	1.98
Gwynn Falls	2.36
Morgan Creek	2.76
Manokin Branch	2.8

3.5. Elevation Effect on Isotopic Composition

There was a significant negative relationship between elevation and the isotope values (Figure 7). The calculated altitude gradients were approximately -0.1‰ for $\delta^{18}\text{O}$ and -0.6‰ for $\delta^2\text{H}$ per 100 m of gain in elevation, confirming an altitude effect where isotopic values become lighter (more negative) at higher elevations.

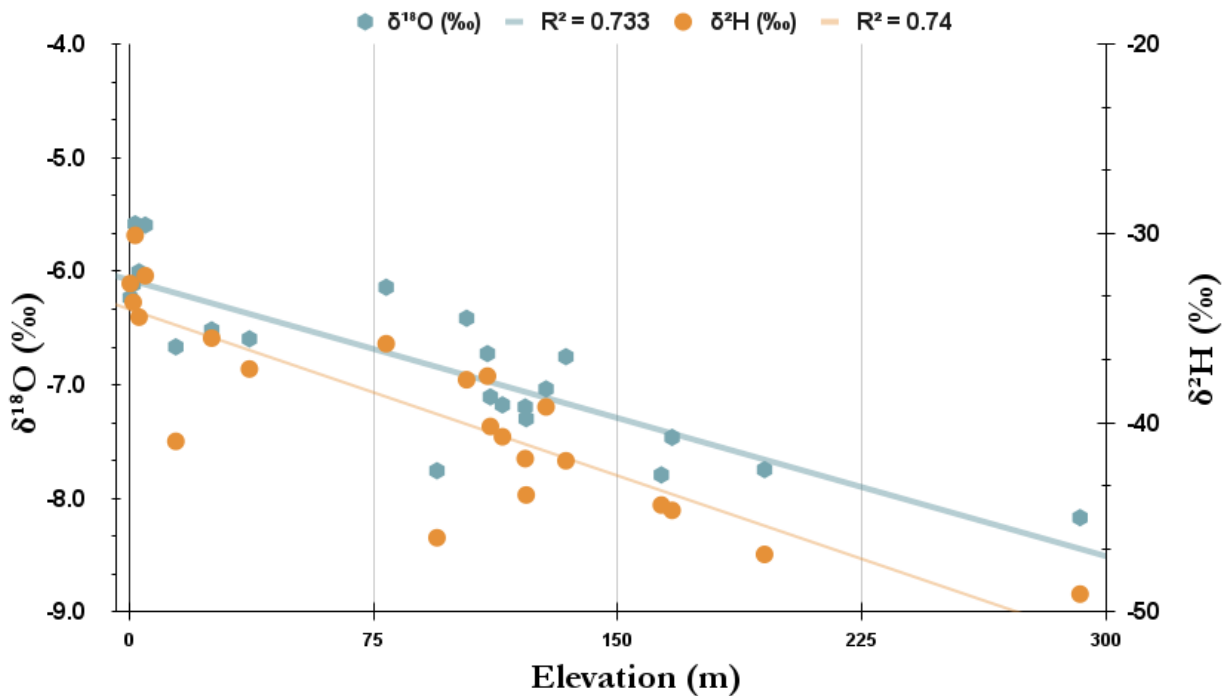


Figure 7. Relationship between elevation and annual average river $\delta^2\text{H}$ and $\delta^{18}\text{O}$ values

A seasonal analysis of $\delta^2\text{H}$ and $\delta^{18}\text{O}$ values in relation to elevation revealed consistent differences between summer and winter months across the 22 study sites. Winter samples (December–February) exhibited lighter $\delta^2\text{H}$ and $\delta^{18}\text{O}$ values, with a more consistent and pronounced negative relationship with elevation, demonstrating a clear altitude effect during the cold season (Figure 8).

In contrast, I observed that summer samples (June–August) showed greater variability and scatter across the elevation gradient, suggesting that the altitude effect is less distinct during the warm season, likely due to additional influences such as evaporation, localized convection, or re-evaporation.

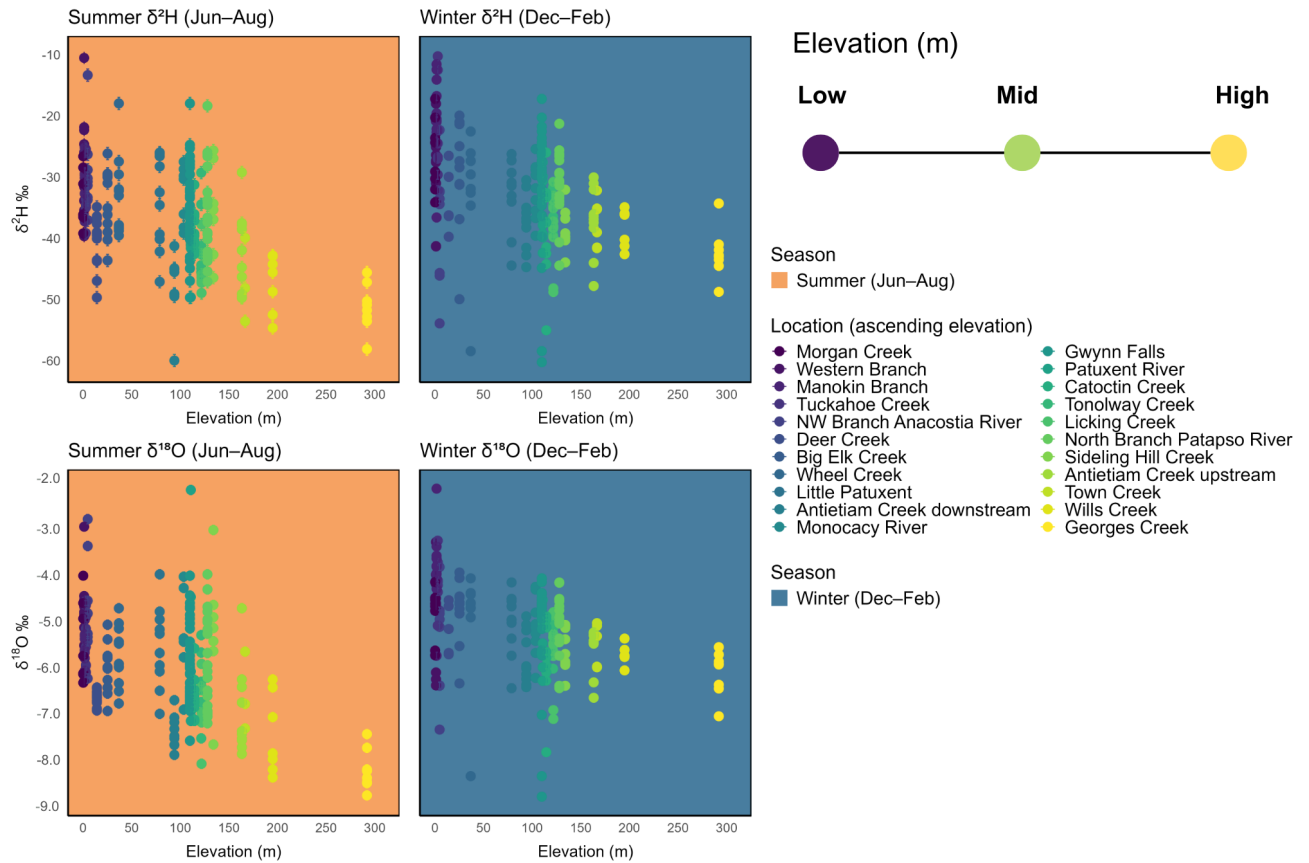


Figure 8. Seasonal variation of $\delta^{18}\text{O}$ and $\delta^2\text{H}$ river values with elevation

3.6. d-excess

The deuterium excess (d-excess) values across Maryland streams varied considerably, with mean values ranging from 12.1 to 16.5‰ and standard deviations differing notably between stations (Table 6; Figure 9). A one-way ANOVA confirmed that differences in mean d-excess values among stations were statistically significant ($p < 0.01$), reflecting spatial variability in underlying hydrological processes such as evaporation intensity, moisture source, or groundwater influence. Streams in western Maryland—such as Georges Creek, Wills Creek, and Sideling Hill Creek—exhibited both higher mean d-excess and lower variability, consistent with long-distance transport of lighter, less evaporatively modified moisture from Great Lakes-fed systems, particularly during winter months. These sites were also located in higher-elevation areas where most of the streamflow comes from groundwater, and minimal surface evaporation, which kept their isotope values more stable. In contrast, streams located in the Piedmont and Coastal Plain, such as the North Branch Patapsco River and Patuxent River, showed heavier and more variable d-excess values, indicative of shorter-range atmospheric recycling and greater evaporative influence—especially in catchments with surface water retention and wetland coverage. Patuxent River within the Piedmont province, showed this pattern with one of the broadest d-excess ranges among all stations. This likely reflects a seasonal shift between evaporatively enriched surface runoff during summer and groundwater recharge contributions in cooler months.

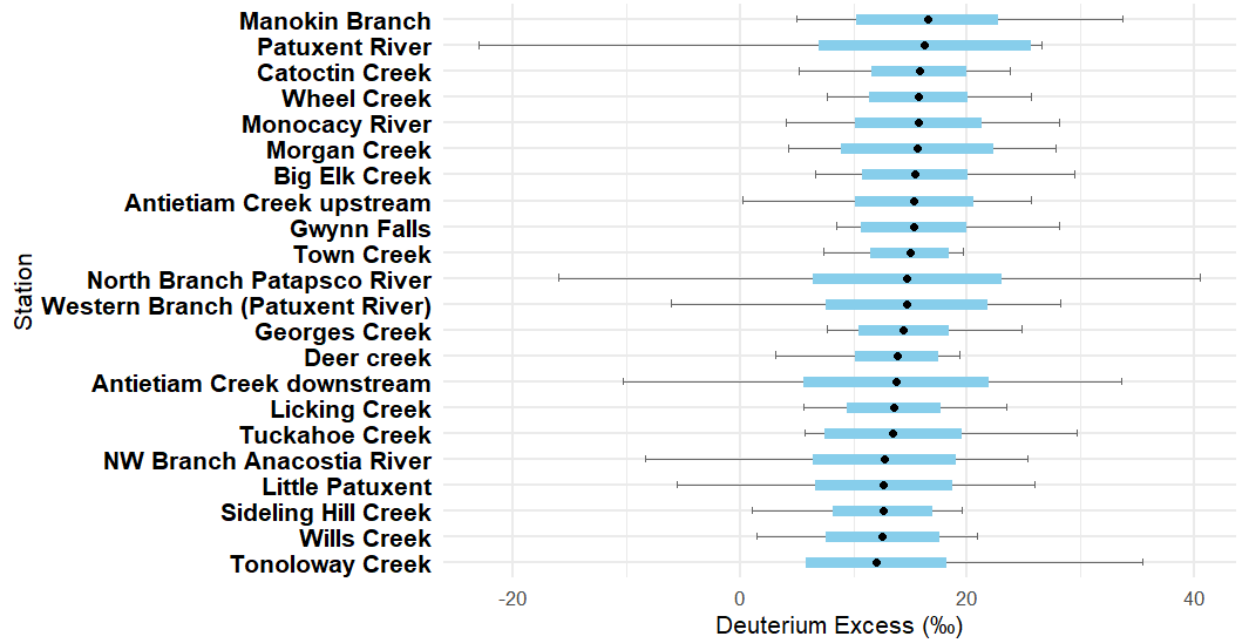


Figure 9. Mean and variability of deuterium excess (*d*-excess) across 22 river and stream stations in Maryland. Black dots represent the mean *d*-excess value at each station, blue bars show the standard deviation, and whiskers indicate the full range of observed values (minimum to maximum)

Table 6. Mean deuterium excess (*d*-excess) values for selected Maryland river and stream sites

Location	Mean deuterium excess
Wills Creek	12.09
Sideling Hill Creek	12.14
Little Patuxent	13.18
NW Branch Anacostia River	13.38
Tonoloway Creek	13.829
Deer Creek	13.88
Licking Creek	13.98
Western Branch	13.96
Town Creek	14.19
Tuckahoe Creek	14.29
Monocacy River	14.97
Wheel Creek	14.96
Antietam Creek (upstream)	15
Patuxent River	15
Georges Creek	15.07
North Branch Patapsco River	15.447
Gwynn Falls	15.58
Big Elk Creek	15.6
Catoctin Creek	15.867

Antietam Creek (downstream)	16.14
Manokin Branch	16.46
Morgan Creek	16.502

3.7. Hydrograph Separation and BFI index

3.7.1 Baseflow Separation Across Physiographic Regions

Hydrograph separation using SepHydro revealed notable variation in baseflow contributions across the five selected river systems, each representing a distinct physiographic province in Maryland (Figure 10). Georges Creek (Appalachian Plateau) exhibited a BFI of ~62.6%, indicating a moderate groundwater contribution, consistent with steep slopes and deeper aquifers supporting delayed subsurface flow. Town Creek (Valley and Ridge) showed a BFI of ~59.9%, reflecting a more responsive hydrologic system with stronger stormflow influence, shaped by the region’s mixed topography and limited infiltration capacity. Catoctin Creek (Blue Ridge) yielded a BFI of ~53.3%, pointing to sustained groundwater inputs, aligned with the fractured bedrock and moderate surface runoff typical of the region. The upper portions of the Patuxent River (Piedmont) displayed a BFI of ~68.3%, suggesting a well-buffered stream system supported by moderate slopes and permeable soils. Meanwhile the Western Branch (of the Patuxent; Coastal Plain) had a BFI of ~43.6%, indicating a predominantly stormflow-driven system, influenced by shallow unconfined aquifers and flat terrain that promotes rapid surface runoff.

3.7.2. Optimal Hydrograph Separation Using Isotopes

The optimized BFI_{max} values derived from isotope calibration were consistently higher than the uncalibrated SepHydro outputs, although the magnitude of adjustment varied by station. For example, Georges Creek showed an increase from a SepHydro BFI of 0.606 to an optimized BFI_{max} of 0.75, with a corresponding RMSE of 0.144—reflecting groundwater input. Town Creek had a smaller difference (0.54 to 0.59; RMSE = 0.051), suggesting closer agreement between the two methods. In contrast, Catoctin Creek and the Patuxent River required more substantial adjustments (0.63 to 0.8 and 0.7 to 0.8, respectively), with RMSE values of 0.167 and 0.117, highlighting a stronger groundwater signal. Western Branch, which had the lowest SepHydro BFI (0.43 to 0.50) and RMSE of 0.164 indicates a limited groundwater signal that was partially but not substantially underestimated by the uncalibrated model, supporting the interpretation that Western Branch is predominantly stormflow-driven (Table 7).

Table 7. Comparison of Sephydro BFI and optimized BFI_{max} with station-specific root mean square error (RMSE) values

Station	SepHydro BFI	Optimized BFI _{max}	RMSE
Georges Creek	0.6	0.75	0.144
Town Creek	0.54	0.59	0.051
Catoctin Creek	0.63	0.8	0.167
Patuxent River	0.7	0.8	0.117
Western Branch	0.43	0.5	0.164

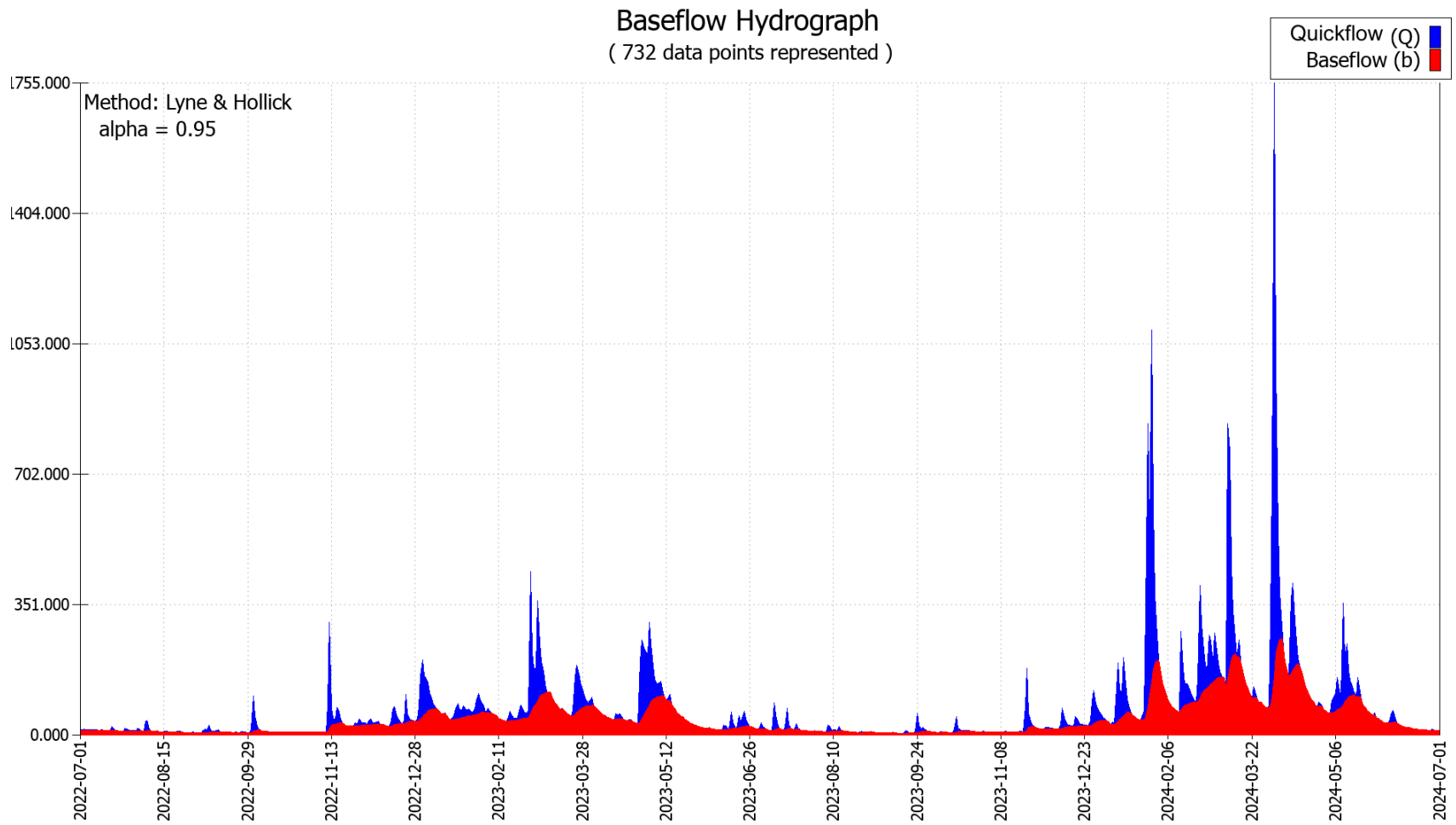
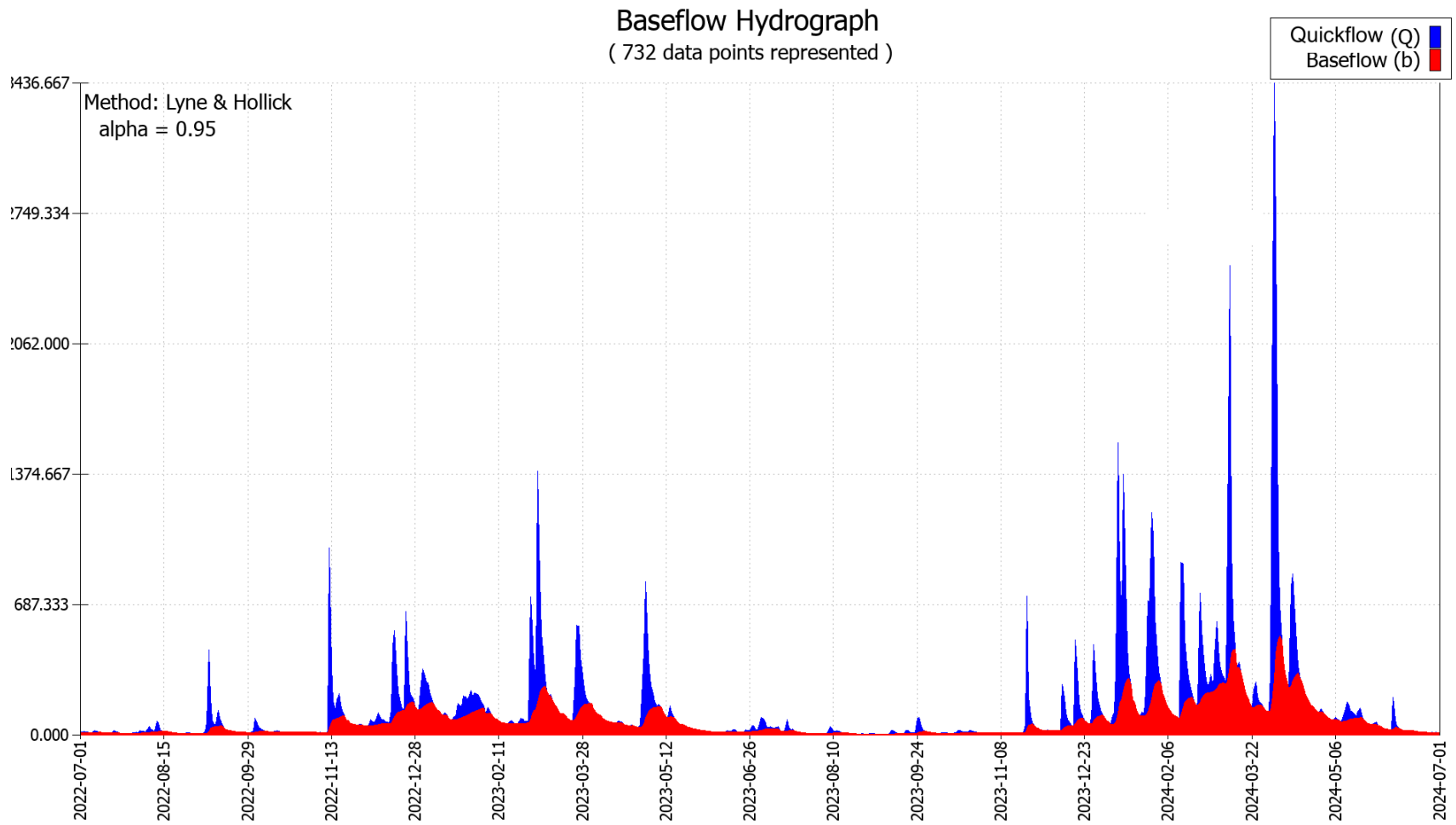
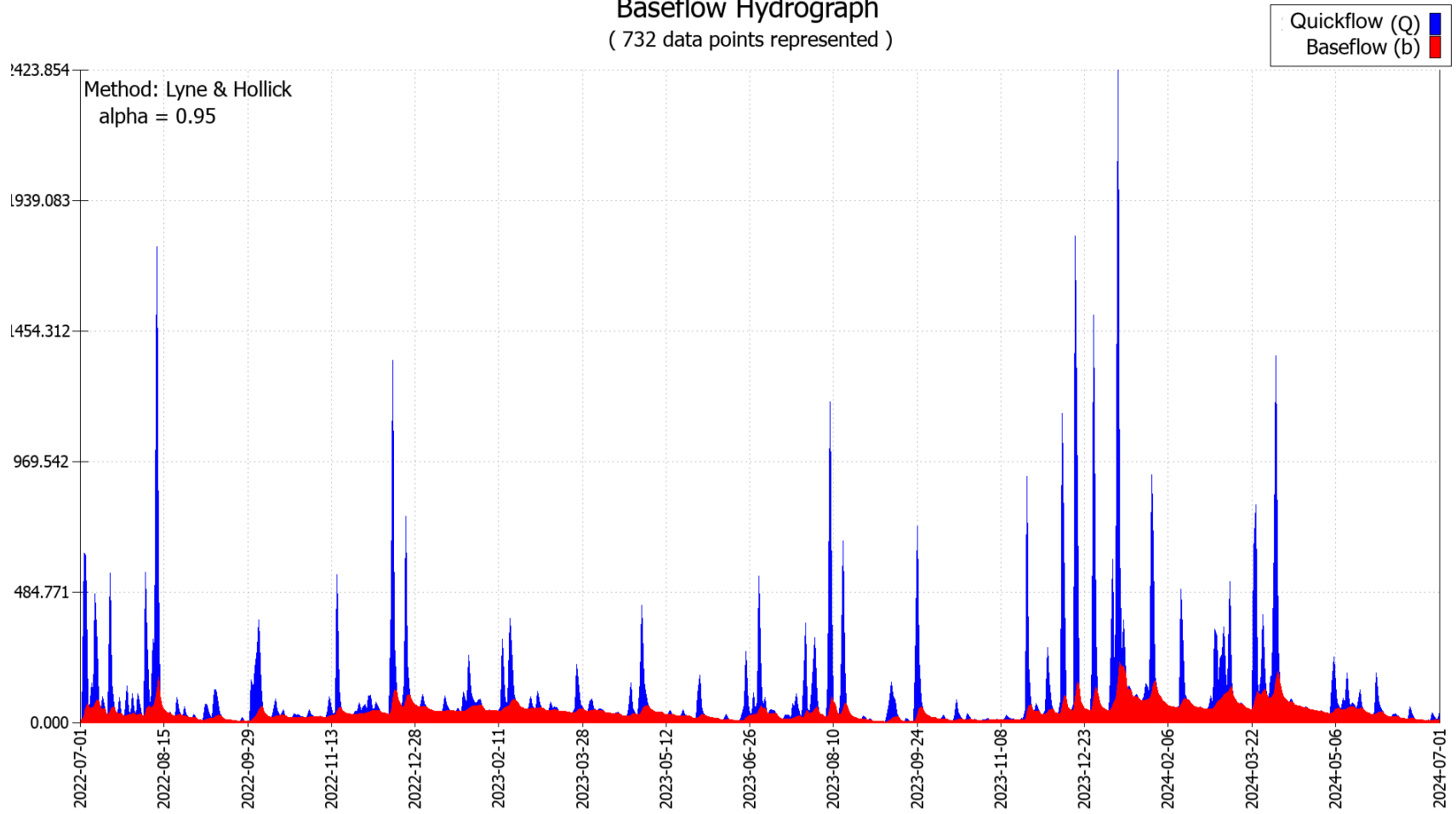


Figure 10. (a) Georges Creek hydrograph (BFI 62.6%)

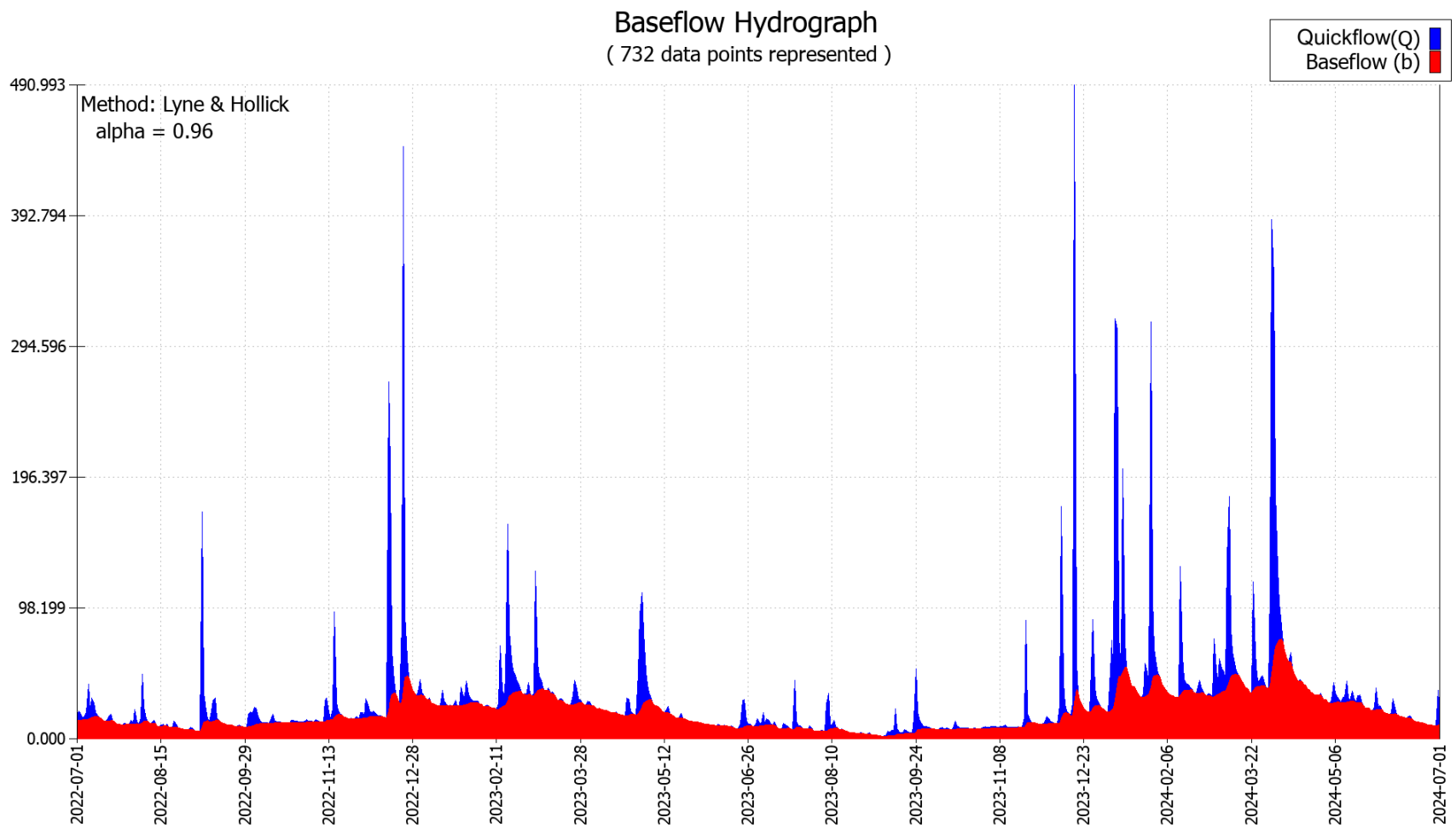


10. (b) Town Creek hydrograph (BFI = 59.9%)

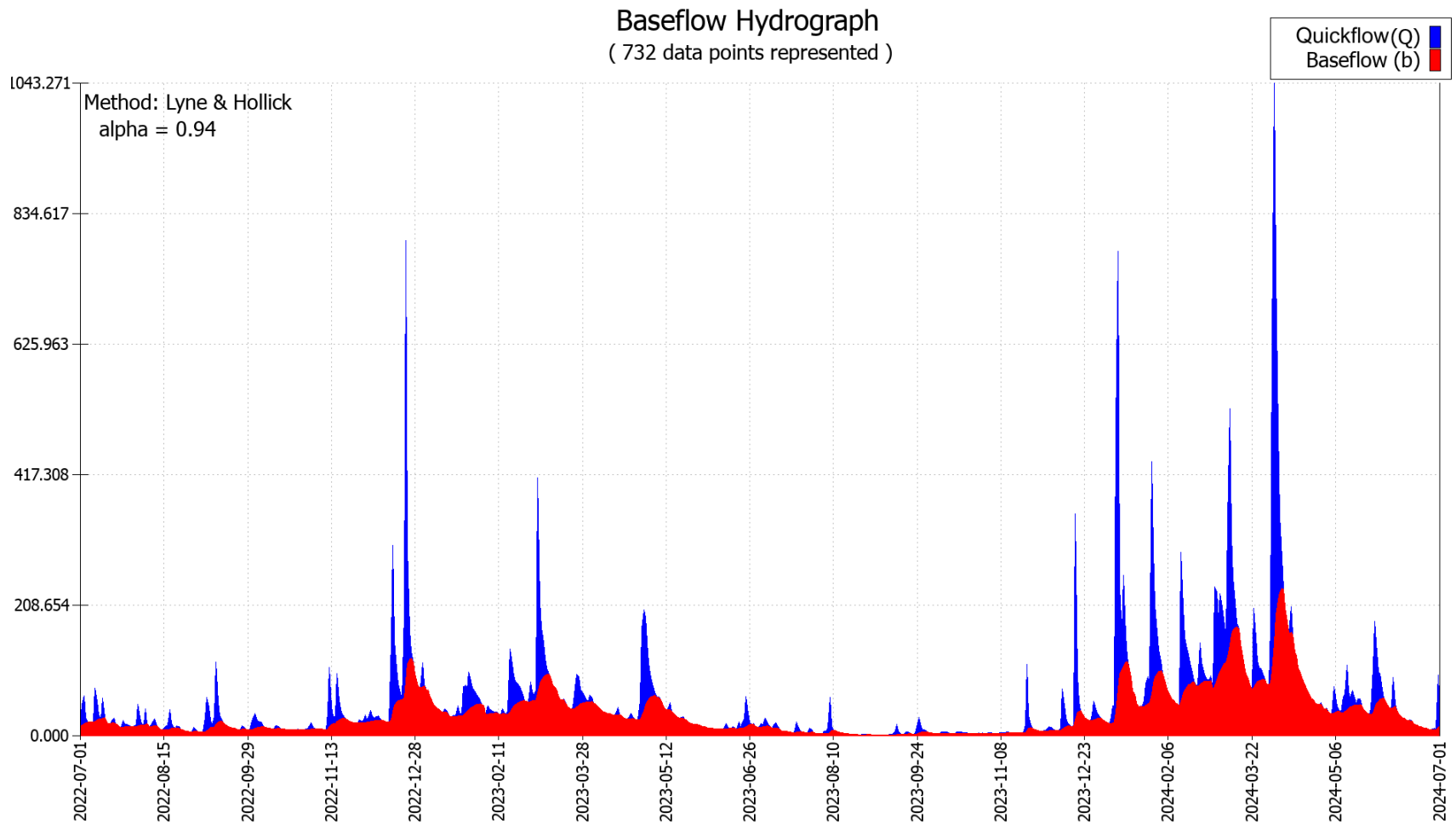
Baseflow Hydrograph (732 data points represented)



10. (c). Western Branch hydrograph (BFI = 43.6%)



10. (d). Patuxent River hydrograph (BFI = 68.3%)



10. (e). Catoctin Creek hydrograph (BFI = 53.3%)

Figure 10. Hydrograph separation of quickflow and baseflow for five stations based on their physiographic variation

3.7.3. Comparison of BFI_{max} and Isotope Composition

There was a very strong relationship ($R^2 = 0.93$) between BFI (determined using SepHydro) and the optimized value of BFI_{max} based on the OHS procedure, although all five BFI_{max} values were higher than their corresponding BFI values (Fig. 11). This result strongly suggests that the stable isotopic data plays an important role in calibrating each hydrograph separation in the same direction (i.e., more baseflow and less direct runoff, on average).

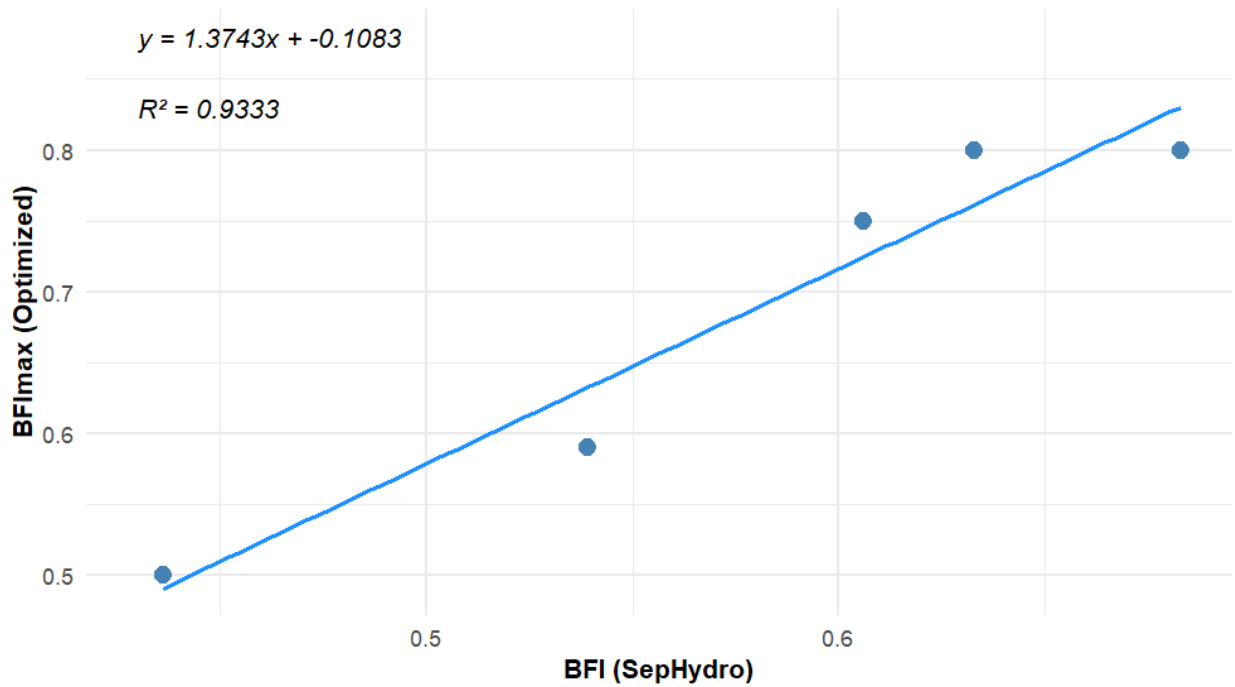


Figure 11. Comparison of SepHydro-derived BFI and optimized BFI_{max} values across five selected watersheds

The plot of BFI_{max} values against average $\delta^2\text{H}$ and $\delta^{18}\text{O}$ values for each station revealed a spatial and hydrological gradient, where rivers with higher BFI_{max} values generally exhibited less negative (i.e., isotopically heavier) delta values—particularly in $\delta^2\text{H}$ (Figure 12). For example, the Western Branch, had the heaviest (least negative) $\delta^2\text{H}$ value (-33.9‰) alongside a BFI_{max} of 0.5, suggesting significant evaporative enrichment and limited groundwater input. In contrast, Georges Creek, draining the Appalachian Plateau, had a higher BFI_{max} of 0.75 but a much lighter $\delta^2\text{H}$ value (-52.6‰), indicative of deeper groundwater flow paths, longer residence times, or snowmelt influence. Interestingly, Town Creek showed a relatively low BFI_{max} (0.59) and also a heavier $\delta^2\text{H}$ signature (-47.4‰), consistent with rapid runoff and storm-dominated flow. These findings suggest that while systems with higher BFI_{max} generally exhibit lower isotope values due to deeper groundwater inputs, this relationship can vary depending on regional geology, aquifer depth, and the extent of surface water exposure to evaporation.

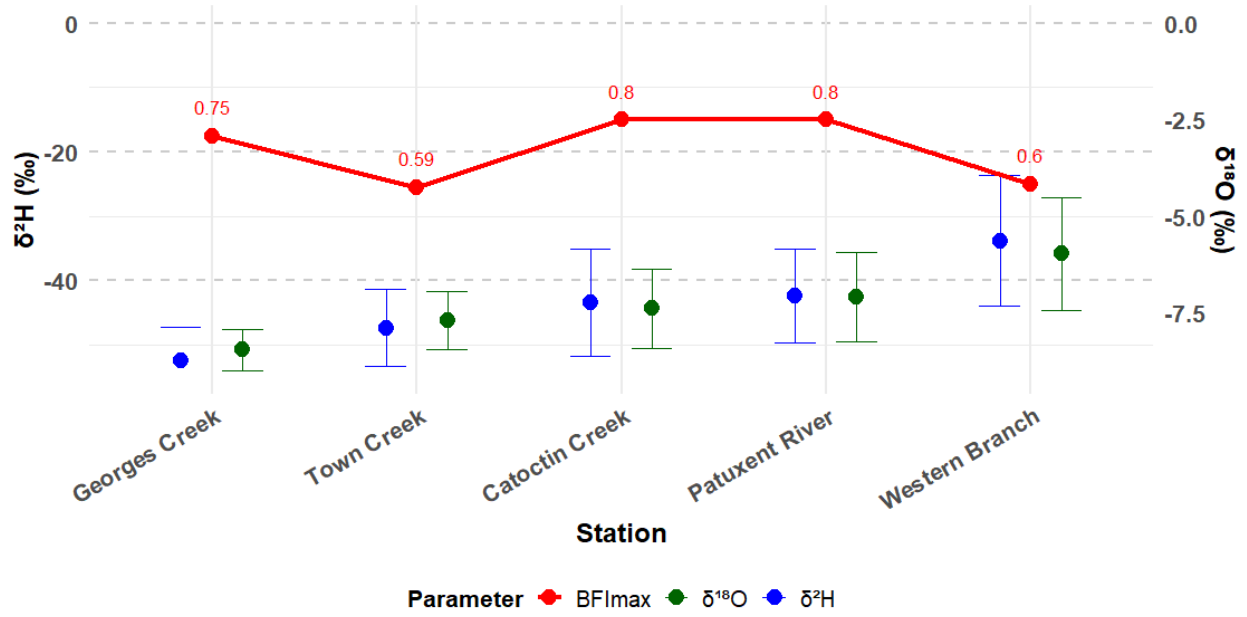


Figure 12. Comparison of SepHydro-derived BFI and optimized BFI_{max} values across five Maryland watersheds

4. Discussion

The isotopic composition of Maryland's rivers and streams is shaped by precipitation sources, regional physiography, and hydrological dynamics. Variability in $\delta^2\text{H}$ and $\delta^{18}\text{O}$ across the 22 study sites reflects the influence of seasonal patterns, watershed scale, and landscape setting. Western Maryland rivers and streams, such as Georges Creek and Wills Creek, located in the Appalachian Plateau and Ridge and Valley provinces, consistently were relatively depleted in heavy isotopes. This pattern is likely influenced in part by moisture that has traveled longer distances inland—undergoing progressive rainout during transport—which contributes to lighter isotopic signatures, as commonly observed in continental regions further from oceanic influence (Table 2, Gat, 1996). Lower temperatures associated with higher altitudes also contribute to these patterns.

By contrast, rivers in the Piedmont and Coastal Plain provinces—including Manokin Branch, Western Branch, and Little Patuxent River—showed higher $\delta^2\text{H}$ and $\delta^{18}\text{O}$ values. These surface waters likely receive a greater proportion of warm-season precipitation and may also reflect evaporative enrichment during summer months, especially in systems with greater overland flow. In winter, however, when much of the warm-season runoff has already reached the estuaries or the ocean, isotopic differences are more likely driven by air temperature and the altitude of recharge. The observed spatial gradients suggest that physiographic factors—such as elevation, watershed size, and terrain complexity—interact with atmospheric transport to shape isotope patterns. These findings indicate that physiography exerts a stronger influence on the isotopic variability. This regional effect on isotopic composition has been similarly observed in prior studies where elevation and moisture source distance significantly affect $\delta^2\text{H}$ and $\delta^{18}\text{O}$ values (Clark & Fritz, 1997; Bowen et al., 2019).

The Local Meteoric Water Line (LMWL) showed a strong linear relationship, indicating that the isotopic composition of river water primarily reflects precipitation inputs with limited evaporative modification (Figure 5). The slight deviation from the GMWL indicates that kinetic fractionation contributes alongside equilibrium processes in shaping the isotopic composition. This deviation suggests the influence of local fractionation processes, such as evaporation or atmospheric moisture recycling, under region-specific conditions. Higher slopes in the LMWL reflect equilibrium fractionation and minimal evaporation. While higher elevations do result in more negative $\delta^2\text{H}$ and $\delta^{18}\text{O}$ values due to rainout and cooling, this shift occurs along the meteoric water line, rather than altering its slope (Rozanski et al., 1993). Similar trends have been observed elsewhere in the northeastern United States, where regional LMWLs deviate from the GMWL due to local climatic conditions. The higher intercept suggests a stronger meteoric input with little to no evaporation, potentially reflecting shifts in moisture sources and atmospheric moisture recycling (Bowen et al., 2019), which aligns with findings in other humid regions but differs from LMWLs in semi-arid locations where evaporation lowers the slope of the line relating $\delta^2\text{H}$ values to $\delta^{18}\text{O}$ values.

Each site's River Water Line (RWL) (Figure 6) and lc-excess values (Table 4) provided useful insight into local hydrological behavior. At Antietam Creek Downstream, the RWL had a shallow slope ($\delta^2\text{H} = 2.8 \cdot \delta^{18}\text{O} - 24.98$), suggesting that the water had isotopic changes likely caused by evaporation or mixing with enriched sources. The lc-excess value (1.18) was slightly positive and showed little variation across samples, indicating that the site water had similar isotope values shaped by evaporation, and didn't vary much from that pattern. This combination of a flat slope and stable lc-excess pointed to conditions where water had stayed at or near the surface for longer periods, allowing more time for evaporation. In contrast, Licking Creek exhibited a relatively high

RWL slope ($\delta^2\text{H} = 6.44 \cdot \delta^{18}\text{O} + 2.19$) and a very low lc-excess value (0.03), indicating strong alignment with meteoric water conditions and minimal evaporative modification. The data points were tightly clustered, showing consistent isotopic signatures typical of baseflow-dominated inputs. The near-zero lc-excess further supports the interpretation that water at this site experienced little fractionation, likely moving efficiently through subsurface pathways.

The comparison between modeled precipitation isotope values and observed river water across Maryland revealed a consistent seasonal pattern. In all physiographic regions, river water showed higher isotope values than winter precipitation and lower values than summer precipitation for both $\delta^2\text{H}$ and $\delta^{18}\text{O}$ (Table 3). This indicated that river water does not reflect the isotope signature of recent precipitation alone but is influenced by seasonally mixed recharge and delayed hydrological response. These isotope values suggested that most stream and river flow is also sustained by groundwater discharge, rather than just direct runoff from recent rainfall. The values likely reflect cool-season recharge, particularly from fall and winter months, when precipitation has a better chance of infiltrating into the subsurface due to reduced evapotranspiration. As river and stream water is not as light as modeled winter precipitation, this may reflect limitations in the OIPC estimates; although OIPC-modeled values tend to assign slightly more negative $\delta^2\text{H}$ and $\delta^{18}\text{O}$ values than field measurements, they capture the broader seasonal trend of winter depletion.

Modeled seasonal precipitation patterns—particularly the balance between cool-season recharge and warm-season deficit—appeared to play a key role in shaping the isotopic composition of stream and river flow. Estimated winter precipitation showed the lowest $\delta^2\text{H}$ and $\delta^{18}\text{O}$ values, while summer precipitation was more enriched in heavy isotopes, consistent with temperature-dependent fractionation and shifts in moisture sources (Figure 4). These seasonal patterns also helped explain the interannual shifts observed in moisture surplus-weighted isotope values in river water. In drier

hydrologic years like 2023–2024, when summer recharge is limited due to higher evaporation and a reduced surplus, stream water was more strongly influenced by groundwater that is recharged by winter precipitation, including snowmelt and cold-season rain. This resulted in lower $\delta^2\text{H}$ and $\delta^{18}\text{O}$ values across most stations (Figure 3). In contrast, 2022–2023 had a higher annual surplus and slightly higher isotope values, suggesting a more balanced contribution from both warm- and cool-season precipitation. Similar seasonal recharge patterns have been reported in regions with temperate climates, such as the Midwestern U.S. (Bedaso & Wu, 2020), where cold-season inputs dominate in dry years due to limited summer infiltration (Simpkins, 1995; Kendall & Coplen, 2001). This differs from monsoon-influenced systems, where summer rainfall typically drives the annual isotopic signal (Singh et al., 2010).

I also observed a clear elevation effect in my results, where higher elevation sites exhibited lower $\delta^2\text{H}$ and $\delta^{18}\text{O}$ values (Figure 7). This pattern aligns with the expected influence of adiabatic cooling and isotopic fractionation during condensation as air masses rise in elevation (Poage & Chamberlain, 2001). Although consistent with global trends, the gradient observed in Maryland is slightly lower than those reported in more topographically extreme regions such as the Andes or Himalayas (Rowley et al., 2001), likely due to Maryland's more moderate elevation range. However, regional humidity may also play a role in moderating isotopic depletion with altitude and could warrant further investigation (Poage & Chamberlain, 2001). Seasonal $\delta^2\text{H}$ and $\delta^{18}\text{O}$ versus elevation plots (Figure 8) highlight the influence of more uniform, long-distance frontal systems during winter, in contrast to more variable, localized convective storms in summer, which introduce greater isotopic variability, particularly at lower elevations.

From the hydrographs, I observed that sites such as Georges Creek and the Patuxent River had smoother recessions and more sustained baseflow, aligning with their moderately high BFI values

and suggesting stronger groundwater influence. In contrast, the Western Branch and Town Creek exhibited steeper hydrograph responses and shorter recession limbs, consistent with lower BFI values and more stormflow-dominated behavior. When comparing SepHydro-derived BFI values with isotope-optimized BFI_{max} values, I determined that BFI_{max} was consistently higher across all sites (Table 7). This discrepancy suggests that SepHydro may underestimate baseflow in systems with prolonged groundwater input or complex subsurface hydrology. The use of isotopic data in calibrating BFI_{max} offers a more integrated and time-averaged understanding of water source contributions, capturing delayed subsurface flow, evaporative effects, and groundwater mixing that may not be reflected in empirical filter-based models. For example, at Western Branch, the optimized BFI_{max} of 0.60 was substantially higher than the SepHydro BFI of 0.436, indicating that even in “flashy” systems, groundwater contributions may be more significant than initially estimated. The graph plotting BFI_{max} against average $\delta^2\text{H}$ and $\delta^{18}\text{O}$ values further supported these interpretations (Figure 11). I observed that stations with higher BFI_{max} values generally exhibited less negative (i.e., heavier) isotope signatures, particularly in $\delta^2\text{H}$, likely due to longer residence times, evaporative enrichment, or shallow aquifer interactions. High BFI_{max} values might be more prevalent in lower-elevation settings where groundwater has longer residence times, flows through shallow aquifers, and is more exposed to evaporative processes—factors that can result in heavier isotope signatures. In contrast, high-elevation sites typically have steeper terrain and limited aquifer storage, promoting faster runoff and contributing to lighter δ -values due to reduced subsurface mixing. In contrast, stations with lower BFI_{max} had more lighter isotopic values, suggesting rapid runoff and limited groundwater mixing. These isotopic patterns aligned closely with physiographic differences: upland systems with fractured bedrock and deeper aquifers (e.g., Appalachian Plateau, Valley and Ridge) tended to show lighter isotope signatures, while lowland

systems with shallow aquifers (e.g., Coastal Plain) were more enriched in heavy isotopes, likely due to stronger evaporative influences, near-surface flow paths and also elevation and temperature effects, as higher-altitude sites receive isotopically lighter precipitation.

D-excess values further supported these interpretations. Across all sites, values consistently exceeded 10‰, ranging from 12.14‰ to 16.14‰ (Figure 9), which aligns with the findings of Kendall and Coplen (2001), who reported similarly positive d-excess values for rivers across the United States. In general, higher d-excess values indicate the addition of re-evaporated moisture into the atmosphere, while lower values are typically associated with samples affected by evaporation from surface water bodies. In western Maryland, elevated d-excess values suggest an influence from long-distance moisture transport, likely originating from cold, high-latitude air masses and the Great Lakes region. In these source areas, kinetic fractionation processes—such as re-evaporation of moisture over relatively warm lake surfaces, particularly Lake Erie—can increase d-excess values (Machavaram & Krishnamurthy, 1995; Gat, 1996). Generically, lake-effect moisture may contribute to the isotopic composition of surface waters observed at some higher-elevation western sites (Bowen & Revenaugh, 2003). In contrast, lower d-excess values in eastern Maryland likely reflect shorter transport pathways and a stronger influence of local moisture. In this region, evaporation from the Chesapeake Bay, estuaries, and low-lying wetlands under warmer and more humid conditions contributes to isotopic fractionation, leaving an imprint of local water bodies on precipitation. Lower d-excess values in eastern Maryland likely reflect shorter atmospheric transport and stronger influence of local moisture recycling and evaporation. This pattern is consistent with previous findings that low d-excess is associated with regions characterized by high humidity and enhanced surface evaporation, where non-equilibrium fractionation dominates moisture fluxes (Pfahl & Sodemann, 2014).

5. Limitations and Future studies

This study has a few limitations that apply to interpreting the results. First, the dataset is constrained to a limited number of sampling sites and comprises only a two-year dataset, which may not fully capture spatial heterogeneity across the entire Maryland watershed network. Additionally, while seasonal trends were examined, longer-term historical datasets would be beneficial for assessing climate-driven isotopic shifts over decadal scales. The precipitation isotope values used for comparison were modeled estimates from OIPC, rather than directly measured data; incorporating observed precipitation isotope measurements in future work would improve the accuracy and reliability of regional hydrological interpretations.

Future research should expand the temporal scope of isotopic data collection to improve understanding of long-term trends and interannual variability in river and stream water isotopic composition. Further investigations should focus on the influence of land use changes, groundwater contributions, and anthropogenic modifications to river systems to distinguish natural isotopic variability from human-induced alterations. This would provide a more comprehensive understanding of how urbanization, agricultural practices, and watershed management strategies impact hydrological and isotopic dynamics. Applying advanced hydrological modeling techniques, particularly isotope-enabled hydrological models, could enhance predictions of isotopic responses to climate variability, land use changes, and extreme weather events. Such models would allow for more robust simulations of hydrological fluxes, precipitation-runoff interactions, and groundwater-surface water exchanges, thereby improving the accuracy of isotopic interpretations.

6. Climate Change impact

Climate change is expected to alter precipitation patterns, temperature regimes, and hydrological processes (Trenberth, 2011), all of which have direct implications for watershed function in Maryland (U.S. EPA, 2016). Stable isotopes provide a valuable tool for assessing these impacts by tracking shifts in precipitation sources, seasonal variability, and evaporation effects in river and stream systems (Kendall & McDonnell, 1998; Jasechko et al., 2016). Projected changes in precipitation seasonality due to climate warming could significantly influence river hydrology (Najjar et al. 2010). For river water in Maryland that is primarily sourced from winter precipitation, an increase in cool-season extreme precipitation events could lead to higher runoff, increased streamflow, and a greater risk of flooding, particularly during periods of high soil moisture saturation. Conversely, reductions in winter precipitation due to shifting storm tracks or decreased snowfall could lead to diminished river recharge and lower baseflow conditions, impacting water availability during dry seasons (Barnett et al., 2005). Such changes can be detected through shifts in the isotopic composition of stream water, particularly in baseflow periods when groundwater contributions dominate. Isotopic tracers help differentiate between precipitation-fed and groundwater-fed systems, offering insight into the relative vulnerability of wetlands and streams to climate variability. For example, wetlands that rely primarily on precipitation may exhibit more variable and enriched isotopic signals under drier conditions, indicating greater sensitivity to climatic shifts (Winter, 2000).

Similarly, warm-season precipitation patterns may also be affected by climate change. If extreme rainfall events become more intense but less frequent, as projected for the mid-Atlantic region, dry soils during warm months may be able to absorb more rainfall, potentially reducing immediate runoff (Kunkel et al., 2013). However, prolonged dry periods between extreme events can lead to

increased evaporative losses in rivers with longer residence times, resulting in higher $\delta^2\text{H}$ and $\delta^{18}\text{O}$ values. This enrichment provides a measurable signature of changing hydrological conditions, allowing isotopes to serve as indicators of altered water balance under shifting climate regimes.

Rivers and streams where $\delta^2\text{H}$ and $\delta^{18}\text{O}$ values remain statistically close to the Global Meteoric Water Line (GMWL) may indicate that residence times are short and evaporative effects are minimal, but climate-induced shifts in precipitation patterns and air temperature could change this balance, leading to more pronounced evaporative effect over time. Additionally, changes in hydrological residence time—driven by change in precipitation duration and intensity—could also impact watershed nutrient dynamics and water quality. Watersheds with short residence times are more sensitive to fluctuations in nutrient inputs, meaning increased runoff events due to climate-driven extreme precipitation could lead to enhanced nutrient transport and potential water quality degradation (Howarth et al., 2006). In contrast, watersheds with longer residence times may experience more gradual changes in nutrient cycling, but reduced groundwater recharge due to declining winter precipitation could lower baseflow contributions, affecting overall water supply. By integrating stable isotope analysis with hydrological and climatic data, future research can provide insights into how Maryland's watersheds will respond to ongoing and future climate changes. Understanding these shifts will be essential for managing flood risks, preserving water quality, and developing climate-adaptive water resource strategies in the region.

7. Conclusion

This study presented a comprehensive isotopic characterization of rivers and streams across Maryland, highlighting how regional patterns in $\delta^2\text{H}$, and $\delta^{18}\text{O}$ values, reflect differences in moisture sources, elevation, seasonality, and atmospheric processes. The isotopic composition of streams and rivers comparing with the modelled precipitation data revealed distinct spatial and temporal signatures, shaped by both large-scale climatic influences and local hydrological conditions.

Cool-season precipitation—particularly snow and winter rain—emerged as a dominant contributor to streamflow in drier years, when reduced summer moisture limits recharge. In these cases, isotopic measurements reflected lower δ -values, consistent with cold-season inputs and longer atmospheric transport paths. In contrast, during the wetter year studied here, with more evenly distributed precipitation, isotopic compositions were less negative, indicating contributions from both cool- and warm-season sources.

Regional differences were also evident as western Maryland sites exhibited more negative $\delta^2\text{H}$ and $\delta^{18}\text{O}$ values and higher d-excess, suggesting influence from long-distance moisture transport, including air masses linked to the Great Lakes and higher-latitude regions. In contrast, eastern sites displayed less negative delta values and lower d-excess, consistent with shorter transport distances and stronger influence of locally recycled moisture.

Overall, the isotopic measurements offered valuable insight into the water sources and atmospheric pathways contributing to river and stream water across Maryland. The findings described the importance of winter precipitation, regional moisture recycling, and elevation in shaping isotope

patterns, providing a baseline for future studies on climate variability, land use change, and hydrological processes in mid-Atlantic watersheds.

References

- Antonia, L.; Paolo, V. Baseflow index regionalization analysis in a Mediterranean area and data scarcity context: Role of the catchment permeability index. *Hydrology and Earth System Science* 2008, 355, 63–75. <https://doi.org/10.1016/j.jhydrol.2008.03.011>
- Antunes, P., Boutt, D. F., & Rodrigues, F. C. (2019). Orographic distillation and spatio-temporal variations of stable isotopes in precipitation in the North Atlantic. *Hydrological Processes*, 33(19), e13362. <https://doi.org/10.1002/hyp.13362>
- Araguás-Araguás, L., Froehlich, K., & Rozanski, K. (2000). Deuterium and oxygen-18 isotope composition of precipitation and atmospheric moisture. *Hydrological Processes*, 14(8), 1341–1355. [https://doi.org/10.1002/1099-1085\(20000615\)14:8<1341::AID-HYP983>3.0.CO;2-Z](https://doi.org/10.1002/1099-1085(20000615)14:8<1341::AID-HYP983>3.0.CO;2-Z)
- Barnett, T. P., Adam, J. C., & Lettenmaier, D. P. (2005). Potential impacts of a warming climate on water availability in snow-dominated regions. *Nature*, 438(7066), 303–309. <https://doi.org/10.1038/nature04141>
- Benettin, P., Volkmann, T. H. M., von Freyberg, J., Frentress, J., Penna, D., Dawson, T. E., and Kirchner, J. W.: Effects of climatic seasonality on the isotopic composition of evaporating soil waters, *Hydrology and Earth System Science*. 22, 2881–2890. <https://doi.org/10.5194/hess-22-2881-2018>
- Bedaso, Z. K., & Wu, Y. (2020). Stable isotope variations of precipitation and implications for climate change. *Hydrological Processes*, 34(1), 150-164. <https://doi.org/10.1016/j.scitotenv.2020.136631>
- Boesch, D. F. (2008). Global warming and the Free State: Comprehensive assessment of climate change impacts in Maryland. Report of the Scientific and Technical Working Group of the Maryland Commission on Climate Change. University of Maryland Center for Environmental Science, Cambridge, MD. Retrieved from <https://ian.umces.edu/publications/global-warming-and-the-free-state-comprehensive-assessment-of-climate-change-impacts-in-maryland/>
- Boesch, D. F., Baecher, G. B., Boicourt, W. C., Cullather, R. I., Dangendorf, S., Henderson, G. R., Kilbourne, H. H., Kirwan, M. L., Kopp, R. E., Land, S., Li, M., McClure, K., Nardin, W., & Sweet, W. V. 2023. Sea-level Rise Projections for Maryland 2023. University of Maryland Center for Environmental Science, Cambridge, MD. Retrieved from <https://www.umces.edu/sea-level-rise-projections>
- Boward, D. M., Kazyak, P. F., Stranko, S. A., Hurd, M. K., & Prochaska, T. P. (1999). From the mountains to the sea: The state of Maryland's freshwater streams. EPA 903-R-99-023. Maryland Department of Natural Resources, Monitoring and Non-tidal Assessment Division, Annapolis, MD. Retrieved from <https://dnr.maryland.gov/streams/Documents/md-streams.pdf>
- Bowen, R. (1986). *Groundwater*. England: Elsevier Applied Science Publishers, 1-2.
- Bowen, G. J., & Revenaugh, J. (2003). Interpolating the isotopic composition of modern meteoric precipitation. *Water Resources Research*, 39(10), 1299. <https://doi.org/10.1029/2003WR002086>
- Bowen, G. J., & Wilkinson, B. H. (2002). Spatial distribution of $\delta^{18}\text{O}$ in meteoric precipitation. *Geology*, 30(4), 315-318. [https://doi.org/10.1130/0091-7613\(2002\)030<0315:SDOIM>2.0.CO;2](https://doi.org/10.1130/0091-7613(2002)030<0315:SDOIM>2.0.CO;2)

- Bowen, G. J., Cai, Z. Y., Fiorella, R. P., & Putman, A. L. (2019). Isotopes in the water cycle: Regional-to-global scale patterns and applications. *Annual Review of Earth and Planetary Sciences*, 47(1), 453–479. <https://doi.org/10.1146/annurev-earth-053018-060220>
- Boicourt, K., & Johnson, Z. P. (Eds.). (2010). Comprehensive strategy for reducing Maryland's vulnerability to climate change: Phase II: Building societal, economic, and ecological resilience. Maryland Commission on Climate Change, Adaptation and Response Working Group. Retrieved March 12, 2025, from https://dnr.maryland.gov/climateresilience/Documents/climatechange_phase2_adaptation_strategy.pdf
- Burns, D. A., McDonnell, J. J., Hooper, R. P., Peters, N. E., Freer, J. E., Kendall, C., & Beven, K. (2002). Quantifying contributions to storm runoff through end-member mixing analysis and hydrologic measurements at the Panola Mountain Research Watershed (Georgia, USA). *Hydrological Processes*, 16(2), 217-235. <https://doi.org/10.1002/hyp.246>
- Cayan, D. R., Das, T., Pierce, D. W., Barnett, T. P., Tyree, M., & Gershunov, A. (2010). Future dryness in the southwest US and the hydrology of the early 21st century drought. *Proceedings of the National Academy of Sciences*, 107(50), 21271–21276. <https://doi.org/10.1073/pnas.0912391107>
- Chesapeake Bay Commission. (2020). The Chesapeake Bay and its watershed: Bay economy. Chesapeake Bay Program. <https://www.chesbay.us/library/public/documents/Fact-Sheets/Bay-Factoids-FINAL.pdf>
- Coplen, T. B., Wildman, J. D., & Chen, J. (1991). Improved preparation of hydrogen for stable isotope ratio analysis. *Analytical Chemistry*, 63(9), 910–912. <https://doi.org/10.1021/ac00009a014>
- Clark, I., & Fritz, P. (1997). *Environmental isotopes in hydrogeology*. CRC Press. Boca Raton, <https://doi.org/10.1201/9781482242911>
- Cleaves, E. T., Edwards, J., & Glaser, J. D. (1989). Geologic map of Maryland. Maryland Geological Survey. http://www.mgs.md.gov/geology/geologic_map/md_geologic_map.html
- Craig, H. (1961). Isotopic variations in meteoric waters. *Science*, 133(3465), 1702–1703. <https://doi.org/10.1126/science.133.3465.1702>
- Craig, H., & Gordon, L. I. (1965). Deuterium and oxygen 18 variations in the ocean and the marine atmosphere. In E. Tongiorgi (Ed.), (pp. 9–130), *Spoletto Meeting on Nuclear Geology, Stable Isotopes in Oceanography Studies and Paleo Temperature: Lab. di Geologia, Pisa*), 9-130.
- Cropper, T. E., Good, S. P., & Migliaccio, K. W. (2021). Comparing deuterium excess to large-scale precipitation recycling models in the tropics. *Hydrological Processes*, 35(4), e14171. <https://doi.org/10.1038/s41612-021-00217-3>
- Danielescu S, MacQuarrie KTB, Popa A (2018) SEPHYDRO: A Customizable Online Tool for Hydrograph Separation. *Groundwater* 56: 589-593. DOI: <https://doi.org/10.1111/gwat.12792>
- Dansgaard, W. (1964). Stable isotopes in precipitation. *Tellus*, 16(4), 436–468. <https://doi.org/10.3402/tellusa.v16i4.8993>

- Dee, S. G., Noone, D. C., Nusbaumer, J., & Bailey, A. (2023). Advances in stable isotope-enabled climate models: A review. *Earth and Space Science*, 10(3), Environ. Res.: Climate 2 022002 <https://doi.org/10.1088/2752-5295/acbbe1>
- Dinçer, T., Al-Mugrin, A., & Zimmermann, U. (1970). Study of the infiltration and recharge through the sand dunes in arid zones with special reference to the stable isotopes and thermonuclear tritium. *Isotopes in Hydrology*. [https://doi.org/10.1016/0022-1694\(74\)90025-0](https://doi.org/10.1016/0022-1694(74)90025-0)
- Douville, H., Raghavan, K., Renwick, J., Allan, R. P., & Arias, P. A. (2021). Water cycle changes. In *Climate Change 2021: The Physical Science Basis*. Intergovernmental Panel on Climate Change (IPCC). <https://www.ipcc.ch/report/ar6/wg1/>
- Dutton, A., Wilkinson, B. H., Welker, J. M., Bowen, G. J., & Lohmann, K. C. (2005). Spatial distribution and seasonal variation in $^{18}\text{O}/^{16}\text{O}$ of modern precipitation and river water across the conterminous USA. *Hydrological Processes*, 19(20), 4121-4146. <https://doi.org/10.1002/hyp.5876>
- Epstein, S., & Mayeda, T. K. (1953). Variation of O^{18} content of waters from natural sources. *Geochimica et Cosmochimica Acta*, 4(5), 213–224. [https://doi.org/10.1016/0016-7037\(53\)90051-9](https://doi.org/10.1016/0016-7037(53)90051-9)
- Foks, S. S., Raffensperger, J. P., Penn, C. A., & Driscoll, J. M. (2019). Estimation of base flow by optimal hydrograph separation for the conterminous United States and implications for national-extent hydrologic models. *Water*, 11(8), 1629. <https://doi.org/10.3390/w11081629>
- Gat, J. R. (1996). Oxygen and hydrogen isotopes in the hydrologic cycle. *Annual Review of Earth and Planetary Sciences*, 24(1), 225-262. <https://doi.org/10.1146/annurev.earth.24.1.225>
- Gat, J. R. (2010). *Isotope hydrology: A study of the water cycle*. London: Imperial College Press
- Gibson, J. J., & Edwards, T. W. D. (2002). Regional water balance trends and evaporation-transpiration partitioning from a stable isotope survey of lakes in northern Canada. *Global Biogeochemical Cycles*, 16(2), 10-1. <https://doi.org/10.1029/2001GB001839>
- GISGeography. (2015). 10 Open Source Remote Sensing Software Packages. Retrieved from <https://gisgeography.com/open-source-remote-sensing-software-packages/>
- Groisman, P. Y., Knight, R. W., & Karl, T. R. (2001). Heavy precipitation and high streamflow in the contiguous United States: Trends in the twentieth century. *Bulletin of the American Meteorological Society*, 82(2), 219-246. [https://doi.org/10.1175/1520-0477\(2001\)082<0219:HPAHSI>2.3.CO;2](https://doi.org/10.1175/1520-0477(2001)082<0219:HPAHSI>2.3.CO;2)
- Halder, J., Terzer, S., Wassenaar, L. I., Araguás-Araguás, L., & Aggarwal, P. K. (2015). The Global Network of Isotopes in Rivers (GNIR): Integration of water isotopes in watershed observation and riverine research. *Hydrological Processes*, 29(3), 580–589. <https://doi.org/10.5194/hess-19-3419-2015>
- Harris, D. C. (2005). *Exploring chemical analysis* (3rd ed.). W. H. Freeman.
- Henderson, A. K., & Shuman, B. N. (2009). Hydrogen and oxygen isotopic compositions of lake water in the western United States. *Geological Society of America Bulletin*, 121(7-8), 1179-1189. <https://doi.org/10.1130/B26441.1>

Holko, L., Demetrovics, J., & Kralik, M. (2023). Isotopic composition of river water: A global synthesis of monitoring networks. *Hydrological Sciences Journal*, 68(3), 345–366. <https://doi.org/10.5194/hess-19-3419-2015>

Howarth, R. W., Anderson, D. B., Cloern, J. E., Elfring, C., Hopkinson, C. S., Lapointe, B., Malone, T., Marcus, N., McGlathery, K., Sharpley, A. N., & Walker, D. (2006). Nutrient pollution of coastal rivers, bays, and seas. *Issues in Ecology*, (7), 1–15.

IPCC. (2014). *Climate change 2014: Impacts, adaptation, and vulnerability*. Intergovernmental Panel on Climate Change. Cambridge University Press, Cambridge.

Jasechko, S., et al. (2016). Global isotope hydrology: Review and prospects. *Hydrological Processes*, 30(1), 19–35.

Jeelani, G., Feddema, J. J., van der Veen, C. J., & Stearns, L. A. (2018). Role of snow and glacier melt in controlling river hydrology in Liddar watershed (western Himalaya) under current and future climate. *Water Resources Research*, 54(6), 3986–4002. <https://doi.org/10.1029/2011WR011590>

Kendall, C., & Caldwell, E. A. (1998). Fundamentals of isotope geochemistry. In C. Kendall & J. J. McDonnell (Eds.), *Isotope tracers in catchment hydrology* (pp. 51–86). Elsevier.

Kendall, C., & Coplen, T. B. (2001). Distribution of oxygen-18 and deuterium in river waters across the United States. *Hydrological Processes*, 15(7), 1363–1393. <https://doi.org/10.1002/hyp.217>

Kunkel, K.E., et al. (2013) Regional Climate Trends and Scenarios for the U.S. National Climate Assessment. Part 3. Climate of the Midwest U.S. NOAA Technical Report NESDIS, 142–143.

Landwehr, J.M., Coplen, T.B., 2006. Line-conditioned excess: a new method for characterizing stable hydrogen and oxygen isotope ratios in hydrologic systems. In: *Proceedings of an International Conference Isotopes in Environmental Studies*, 25–29 October 2004. Monaco, IAEA-CN-118/56, pp. 132135.

Lyne V., Hollick M. (1979) - Stochastic time-variable rainfall-runoff modelling. Institute of Engineers Australia National Conference. Publ. 79/10, pp. 89-93.

Maryland Department of Natural Resources. (2006). DNR @ work: Annual report 2005–2006. https://dnr.maryland.gov/Documents/2005-2006_annualreport.pdf

Maryland Department of Natural Resources. (2019). Non-Tidal Network (NTN) quality assurance project plan: 2019-2020. Maryland Department of Natural Resources. Retrieved from https://dnr.maryland.gov/waters/cbnerr/Documents/NTN-QAPP_2019-2020.pdf

Maryland Department of Natural Resources. (2023). Quality Assurance Project Plan for the Non-tidal Network Program: Nutrient and Sediment Load and Trend Monitoring. Publication # DNR 12-072823-1. Retrieved from https://dnr.maryland.gov/waters/cbnerr/Documents/NTN_QAPP_2023.pdf

Maryland State Climatologist Office. (n.d.). Maryland climate information. University of Maryland. <http://metosrv2.umd.edu/~climate/>

McGuire, K. J., & McDonnell, J. J. (2007). Stable isotope tracers in watershed hydrology. In R. H. Michener & K. Lajtha (Eds.), *Stable isotopes in ecology and environmental science* (2nd ed., pp. 334–374). Blackwell Publishing.

- McGill, L. M., Steel, E. A., Brooks, J. R., Edwards, R. T., & Fullerton, A. H. (2020). Elevation and spatial structure explain most surface-water isotopic variation across five Pacific Coast basins. *Journal of Hydrology*, 583, 124589. <https://doi.org/10.1016/j.jhydrol.2020.124610>
- Morgan, R. P., & Cushman, S. F. (2005). Urbanization effects on stream fish assemblages in Maryland, USA. *Journal of the North American Benthological Society*, 24(3), 643–655. <https://doi.org/10.1899/04-019.1>
- Mote, P. W., Hamlet, A. F., Clark, M. P., & Lettenmaier, D. P. (2005). Declining mountain snowpack in western North America. *Bulletin of the American Meteorological Society*, 86(1), 39–49. <https://doi.org/10.1175/BAMS-86-1-39>
- Najjar, R. G., Walker, H. A., Anderson, P. J., Barron, E. J., Bord, R. J., Gibson, J. R., & Kennedy, V. S. (2010). Potential climate-change impacts on the Chesapeake Bay. *Estuarine, Coastal and Shelf Science*, 86(1), 1-20. <https://doi.org/10.1016/j.ecss.2009.09.026>
- Peng, H., Mayer, B., Harris, S., & Krouse, H. R. (2004). A 10-yr record of stable isotope ratios of hydrogen and oxygen in precipitation at Calgary, Alberta, Canada. *Tellus B*, 56(2), 147-159. <https://doi.org/10.1111/j.1600-0889.2004.00094.x>
- Peel, M. C., Finlayson, B. L., & McMahon, T. A. (2007). Updated world map of the Köppen-Geiger climate classification. *Hydrology and Earth System Sciences*, 11(5), 1633-1644. <https://doi.org/10.5194/hess-11-1633-2007>
- Pfahl, S., & Sodemann, H. (2014). What controls deuterium excess in global precipitation? *Climate of the Past*, 10(2), 771–781. <https://doi.org/10.5194/cp-10-771-2014>
- Poage, M. A., & Chamberlain, C. P. (2001). Empirical relationships between elevation and the stable isotope composition of precipitation and surface waters: Considerations for studies of paleoelevation change. *American Journal of Science*, 301(1), 1-15. <https://doi.org/10.2475/ajs.301.1.1>
- Reckerth, A., Stichler, W., Schmidt, A., Stumpp, C., Čermák, J., & Kučera, J. (2017). Long-term data set analysis of stable isotopic composition in German rivers. *Journal of Hydrology*, 552, 718–731. <https://doi.org/10.1016/j.jhydrol.2017.07.022>
- Reger, J. P., & Cleaves, E. T. (2008). Physiographic map of Maryland and open-file report 08-03-1. Maryland Geological Survey. http://www.mgs.md.gov/geology/physiographic_map.html
- Rohling, E. J. (2013). Oxygen isotope composition of seawater. In S. A. Elias (Ed.), *The encyclopedia of quaternary science* (Vol. 2, pp. 915–922). Elsevier.
- Rosa, E., Hillaire-Marcel, C., Hélie, J.-F., & Myre, A. (2016). Processes governing the stable isotope composition of water in the St. Lawrence River system, Canada. *Isotopes in Environmental and Health Studies*, 52(4–5), 370–379. <https://doi.org/10.1080/10256016.2015.1135138>
- Rowley, D. B., Pierrehumbert, R. T., & Currie, B. S. (2007). A new approach to stable isotope-based paleoaltimetry: Implications for paleoaltimetry and paleohypsometry of the High Himalaya since the Late

Miocene. *Earth and Planetary Science Letters*, 188(1-2), 253-268. [https://doi.org/10.1016/S0012-821X\(01\)00324-7](https://doi.org/10.1016/S0012-821X(01)00324-7)

Seager, R., Ting, M., Held, I., Kushnir, Y., Lu, J., Vecchi, G. & Naik, N. (2007). Model projections of an imminent transition to a more arid climate in southwestern North America. *Science*, 316(5828), 1181–1184. <https://doi.org/10.1126/science.1139601>

Singh, B. P., & Kumar, B. (2005). *Isotopes in hydrology, hydrogeology and water resources*.

Sodemann, H. (2006). *Stable Isotopes of Water: Processes and Applications*, Chapter 2, In: Diss. ETH No. 16623, Tropospheric transport of water vapour: Lagrangian and Eulerian perspectives, ETH Zurich.

Swenson, S., & Wahr, J. (2006). Estimating large-scale precipitation minus evapotranspiration from GRACE satellite gravity measurements. *Journal of Hydrometeorology*, 7(2), 252-270. <https://doi.org/10.1175/JHM478.1>

Trenberth, K. E. (2011). Changes in precipitation with climate change. *Climate Research*, 47(1–2), 123–138. <https://doi.org/10.3354/cr00953>

U.S. Geological Survey. (2025). *National Water Information System: USGS water data for the Nation*. <https://waterdata.usgs.gov/nwis>

University of Maryland, Center for Disaster Resilience. (2018). *Maryland climate resilience indicators and scoring system*. University of Maryland. Retrieved from <https://cdr.umd.edu/>

University of Maryland State Climate Office. (2024). *Maryland Climate Summary: Winter 2023–24*. Department of Atmospheric and Oceanic Science, University of Maryland. https://www2.atmos.umd.edu/~climate/Bulletin/bulletin_mdscowin24.pdf

U.S. Environmental Protection Agency. (2016, August). *What climate change means for Maryland* (EPA 430-F-16-022). <https://19january2017snapshot.epa.gov/sites/production/files/2016-09/documents/climate-change-md.pdf>

Walsh, J. E., Wuebbles, D. J., Hayhoe, K., Kossin, J. P., Kunkel, K. E., Stephens, G. L., & Somerville, R. C. (2014). Our changing climate. *Climate Change Impacts in the United States: The Third National Climate Assessment*, 19-67. <https://doi.org/10.7930/J0KW5CXT>

Wels, C., Cornett, R. J., & Lazerte, B. D. (1991). Hydrograph separation: A comparison of geochemical and isotopic tracers. *Journal of Hydrology*, 122(1–4), 253–274. [https://doi.org/10.1016/0022-1694\(91\)90181-G](https://doi.org/10.1016/0022-1694(91)90181-G)

Winter, T. C. (2000). The vulnerability of wetlands to climate change: A hydrologic perspective. *Journal of the American Water Resources Association*, 36(2), 305–311. <https://doi.org/10.1111/j.1752-1688.2000.tb04270.x>